Chapter 3

A sequence-specific DNA binding small molecule triggers the release of immunogenic signals and phagocytosis in a model of B-cell lymphoma

The text of this chapter is taken in part from a manuscript co-authored with Peter B. Dervan (California Institute of Technology).

Abstract

Means to cause an immunogenic cell death could lead to significant insight into how cancer escapes immune control. In this study, we screened a library of five Py-Im polyamides coding for different DNA sequences in a model of B cell lymphoma for the upregulation of surface calreticulin, a pro-phagocytosis signal implicated in immunogenic cell death. We found that hairpin polyamide **1** triggers the release of the Damage-Associated Molecular Patterns (DAMPs) calreticulin, ATP, and HMGB1 in a slow necrotic-type cell death. Consistent with this signaling, we observed an increase in the rate of phagocytosis by macrophages after the cancer cells were exposed to polyamide **1**. The DNA sequence preference of polyamide **1** is 5'-WGGGTW-3' (where W=A/T), indicated by the pairing rules and confirmed by the Bind-n-Seq method. The close correspondence of this sequence with the telomere-repeat sequence suggests a potential mechanism of action through ligand binding at the telomere. This study reveals a chemical means to trigger an inflammatory necrotic cell death in cancer cells.

3.1 Introduction

Avoidance of immune destruction has been called the seventh hallmark of cancer.[1,2] According to the immuno-editing paradigm, the immune system recognizes and destroys those proto-oncogenic lesions capable of triggering an immune response while those that escape immune control grow to become clinically detectable disease.[3-6] Studies suggest that therapies that enlist the immune system maintain more durable disease control in the clinical setting.[7] Chemical methods to cause immunogenicity in cancer cells would be an important tool towards understanding immunomodulation in the treatment of cancer. A prerequisite for the activation of an anti-cancer immune response is the recognition of the damaged cells as a threat. Damaged cells release immunostimulatory molecules, called Damage-Associated Molecular Patterns (DAMPs), to recruit and activate professional phagocytes such as macrophages and dendritic cells.[8-10] These antigen-presenting cells engulf and process the cancer cells to further prime the immune system for targeted elimination of cancer.[11]

While most chemotherapeutic regimens cause a non-immunogenic or even tolerogenic cell death, recent reports suggest anthracyclins or γ-radiation are particularly effective because they result in the release of DAMPs.[9,12] The extracellular exposure of the intracellularly abundant molecules calreticulin (CRT), HMGB1, and ATP have been suggested to form a spatiotemporal code for immunogenicity.[13,14] The presentation of CRT, an abundant ER-resident chaperone protein, to the cell surface was identified as a necessary and sufficient pro-phagocytic signal for professional phagocytes.[9] The study

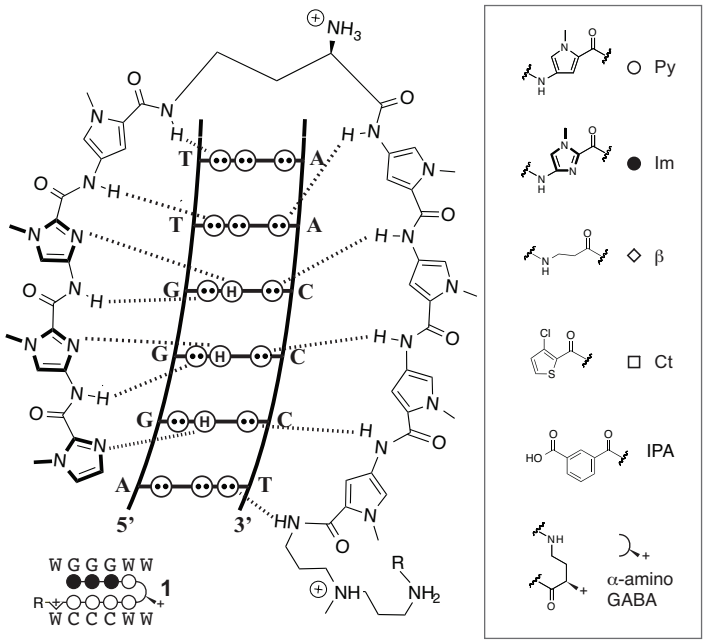

Figure 3.1 Py-Im polyamide recognition of DNA minor groove and corresponding ball-and-stick notation.

showed that stimulation of CRT surface expression by anthracyclins or adsorbtion of the calreticulin protein on the cell surface was sufficient to elicit an anti-cancer immune response in syngeneic mice.[9] Weissman and coworkers further demonstrated in the Raji cell line, a model of human B cell non-Hodgkin's lymphoma, that CRT is the dominant pro-phagocytosis signal that is necessary for engulfment by human macrophages. [15] Furthermore, ATP released from the cytosol into the local microenvironment serves as a lymphocyte recruiting and activating chemokine.[16,17] Lastly, the nucleus-resident protein HMGB1 can be secreted into the surroundings as an inflammatory adjuvant and was shown to be necessary for a durable anti-cancer response in mice.[18,19] Identification of additional small molecules that trigger the release of these DAMPs from tumor cells would be of utility to the field in addressing the heterogeneity of cancers. We became interested in expanding the examined chemical space for compounds capable of causing an immunogenic cell death. Because the DNA damage pathway has been implicated in

immunogenic signaling[20] and anthracyclins are DNA-intercalating ligands, we sought to explore a class of minor groove DNA-binding oligomers hitherto not studied for this biological activity.

Hairpin pyrrole-imidazole (Py-Im) polyamides are a class of sequence-specific oligomers that bind in the minor groove of DNA.[21-26] Sequence preference is achieved by the pair-wise, co-facial arrangement of aromatic amino acids that distinguish the edges of the four Watson-Crick base pairs (Figure 3.1A).[27] Pairing rules for programmable specificity have been established: Im/Py specifies a G•C base pair, Hp/Py codes for T•A base pairs, and Py/Py binds both T•A/A•T. [24] Eight-ring hairpin polyamides are linked in an antiparallel fashion by a central aliphatic γ-aminobutyric acid unit.[28] Polyamides of this hairpin architecture have affinities for match sites similar in magnitude to natural DNA binding proteins (K_a = 10^8 to 10^{10} M^{-1}).[29] Eight-ring hairpins of this class are cell-permeable and modulate transcription in both cells and mice.[30-33] In this study, we screened a small library of Py-Im polyamides coding for different six base pair DNA sequences in Raji cells for the upregulation of surface calreticulin. We found one hairpin polyamide which displayed activity in this screen and characterize its potential for causing an immunogenic cell death.

3.2 Results

Polyamide 1 upregulates calreticulin on the cell surface.

We tested five Py-Im polyamides (**1-5**, Figure 3.2) that bind five unique DNA

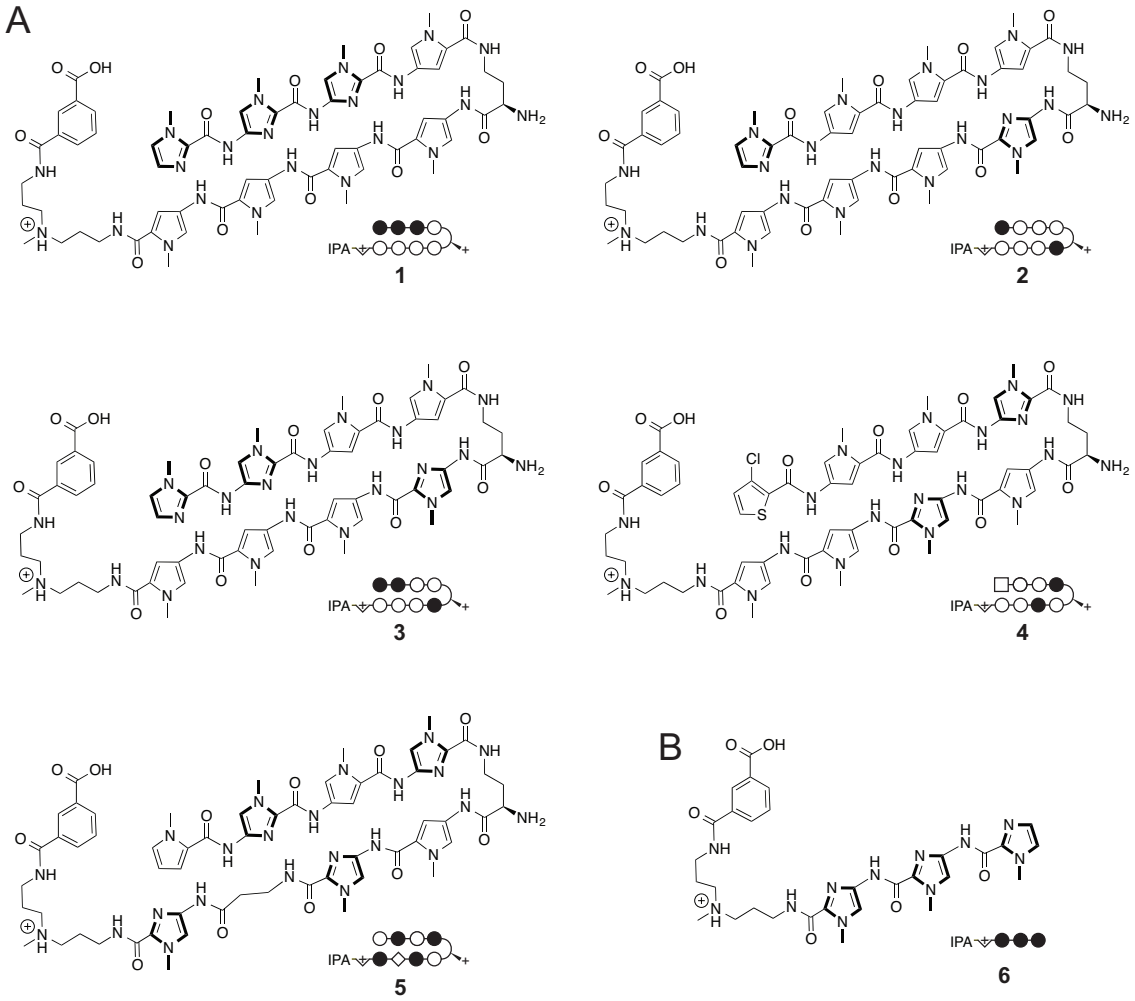

Figure 3.2 A) Structures of hairpin Py-Im polyamides **1-5** screened for stimulation of surface calreticulin (CRT) in Raji cells. B) Structure of ImImIm trimer polyamide **6**.

sequences (5'-WGGGWW-3', 5'-WGWWCW-3', 5'-WGGWCW-3', 5'-WTWCGW-3', and 5'-WCGCGW-3', respectively, where W=A/T) and have demonstrated biological activity.[30,31,34-36] Raji cells, which have previously been utilized in CRT, phagocytosis, and immunotherapy animal models, were dosed at 5 μM for 24 hours with each of the polyamides **1-5**. In addition, 5 μM doxorubicin (**Dox**) and mitoxantrone (**Mtx**, 1 μM) were included as representative anthracyclins. The topoisomerase inhibitor etoposide (**Eto**, 30 μM) was also included for comparison. A 4 hour exposure time point was used

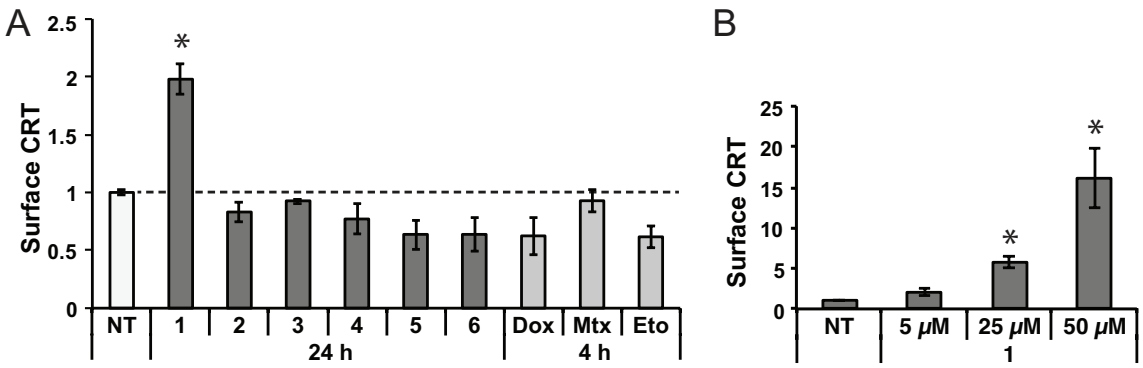

Figure 3.3 A) Surface expression of calreticulin measured by flow cytometry, median fluorescence normalized to non-treated control (NT). Cytotoxic controls doxorubicin (**Dox**, 5 μM), mitoxantrone (**Mtx**, 1 μM), and etoposide (**Eto**, 30 μM). B) Dose-dependence of cell surface CRT to polyamide **1** was measured by flow cytometry after 24 h treatment. Measurement and standard deviation is in triplicate and representative of two independent experiments; asterisk indicates $p<0.05$ by two-tailed Student's t-test compared to NT.

to measure CRT due to the high toxicity of these chemotherapeutics and to be in the range of literature precedent.[9] We measured surface CRT by flow cytometry in a population gated for live cells and saw a statistically significant, two-fold increase in cells treated with only polyamide **1** (Figure 3.3A). In contrast, we saw no activity with the other polyamides **2**-**5** despite their structural similarity. Notably, polyamide **2** has been the most extensively studied amongst this class and has shown activity in prostate cancer xenograft models and the DNA damage response.[33,37] Remarkably, polyamides **3** and **1** share the same molar weight and composition of Im/Py pairs, and only differ by the exchange of one Im/Py ring pair. To assess the structure activity relationship of the imidazole trimer portion of the hairpin oligomer **1**, we synthesized and examined ImImIm polyamide **6**. This was tested because imidazoles are known to complex with calcium and CRT is involved in calcium homeostasis.[38] We did not, however, observe an increase of CRT with polyamide **6**, which suggests the imidazole trimer alone is not sufficient to trigger the surface expression of CRT. We observed no increase in CRT with the two anthracyclins tested, **Dox** and **Mtx**, or with **Eto**. The diminished response to

anthracyclin treatment in Raji cells, as compared to that reported in the literature with murine colon cancer cells, reflects a known range of CRT response to anthracyclins and may be attributable to a difference in cell lines.[39,40] We next increased the treatment concentration of **1** to 25 and 50 μM and found that CRT exposure increased in a dose-dependent manner (Figure 3.3B). The results indicate polyamide **1** is unique in our small library of compounds in its modulation of surface expression of CRT.

Polyamide 1 preferentially binds the sequence 5'-WGGGTW-3'

Py-Im polyamides are a class of sequence-specific DNA-binding ligands and the DNA binding preferences of polyamide **1** may be related to a mechanism of action. By the pairing rules, polyamide **1** is a perfect match to 5'-WGGGWW-3', not unlike the TTAGGG-repeat sequence found in human telomeres. Indeed, dye-conjugated tandem hairpin Py-Im polyamides that recognize 10 base pairs of this repeat sequence can be used to stain telomeres in permeabilized cells.[41,42] We sought to confirm the preferred binding sequence motif of **1** using the Bind-n-Seq method. Bind-n-Seq couples affinity enrichment with next-generation sequencing to query genome-sized sequence space for high-affinity binding sequences.[43] We modified polyamide **1** at the C-terminal position with a biotin-label to afford **1b** (Figure 3.4A) for submission to Bind-n-Seq. Polyamide **1b** strongly preferred binding the DNA sequence motif of 5'-WGGGTW-3' (Figure 3.4B). We additionally confirmed the affinity of polyamide **1** for this sequence by measuring the thermal stabilization afforded to sequence-matched double-stranded DNA.[44] We tested a DNA fragment that included the telomeric DNA sequence

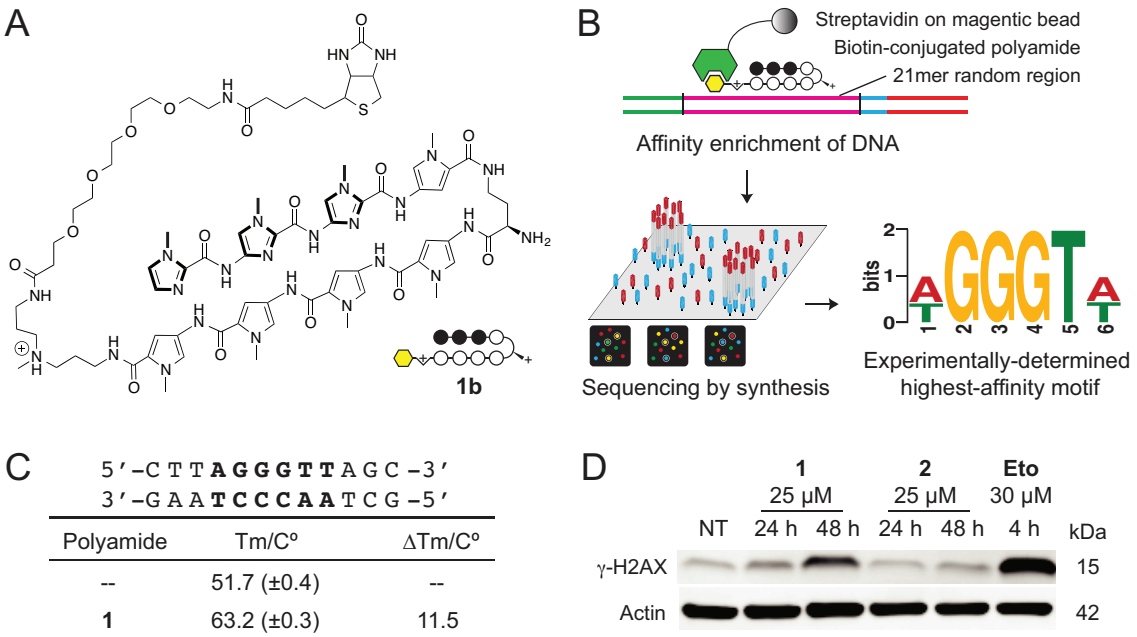

Polyamide	Tm/C°	ΔTm/C°
--	51.7 (±0.4)	--
1	63.2 (±0.3)	11.5

Figure 3.4 Preferred DNA binding sequence of polyamide **1**. A) Structure of polyamide **1b**, the biotinylated analog of **1**. B) Polyamide **1b** was tested by the Bind-n-Seq assay and found to preferentially bind the described DNA sequence motif. C) Affinity of **1** was assessed by a DNA thermal stabilization assay against dsDNA containing the telomeric-repeat sequence 5'-TTAGGG-3'. D) Immunoblot of γ-H2AX and actin control after the indicated treatment.

5'-TTAGGGTTAG-3' (Figure 3.4C). Polyamide **1** stabilized the 12 base pair DNA fragment by 11.5 ºC, suggesting a high affinity hairpin polyamide. Lastly, we detected a marker of DNA stress, phosphorylation of serine 139 on the histone H2AX, after treatment with polyamide **1** but not **2** (Figure 3.4D). We chose the 25 μM dose for this experiment and others described below because it resulted in a robust six-fold increase in surface CRT. We posit that the CRT effect may be due to the unique properties of the DNA target sequence of polyamide **1** in cell biology. The DNA stress, thermal denaturation, and Bind-n-Seq results together suggest the telomere sequence is a plausible target for the mechanism of action of polyamide **1**-mediated CRT exposure.

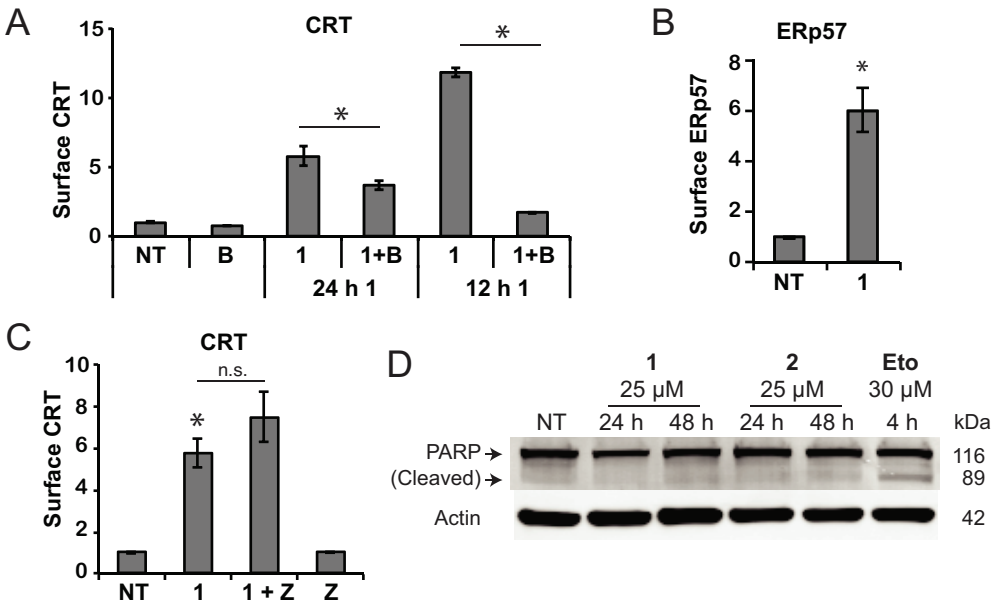

Figure 3.5 Treatment of Raji cells with polyamide **1** triggers anterograde CRT transport by a different mechanism than previously reported for anthracyclins. A) Surface CRT was measured by flow cytometry after Raji cells were treated with 25 μM polyamide **1** for 12 or 24 h and Brefeldin A (**B**) for the final 12 h. B) Co-chaperone ERp57 was measured on the cell surface by flow cytometry after 24 h treatment with **1** at 25 μM. C) Caspase inhibitor Z-VAD-fmk (**Z**, 10 μM) and polyamide **1** (25 μM) were dosed together for 24 h and assessed by flow cytometry for surface CRT. D) Immunoblots for PARP cleavage and actin control after the indicated treatments are shown. All flow cytometry analyses were done in triplicate and are representative of at least two independent experiments. Error bars show standard deviations and asterisks mark statistically significant changes ($p<0.05$) by two-tailed Student's t-test compared to no treatment (unless another comparator is marked).

Polyamide 1 triggers CRT in a different manner than do anthracyclins

To better understand the effects of polyamide **1**, we compared its trigger of CRT to reports of CRT induction by anthracyclins.[45] Anthracyclin-induced CRT exposure has been described to occur with the co-chaperone ERp57 by anterograde ER-Golgi transport.[45] To interrogate whether polyamide **1** induces CRT export to the cell surface by ER-Golgi transport, we applied the Golgi transport inhibitor Brefeldin A[46] (**B**) to Raji cells (Figure 3.5A). Due to the toxicity of **B**, we could only dose **B** for 12 hours. With 24 hour treatment with polyamide **1** and 12 hour treatment with **B**, we saw statistically

significant reduction of CRT on the cell surface when compared to polyamide **1** treatment alone (Figure 3.5A). When polyamide **1** and **B** were dosed together for 12 hours, we saw near ablation of all polyamide **1**-induced CRT, demonstrating the necessity of this pathway for transport. This further suggests CRT has a half-life on the cell surface of at least 12 hours. We additionally measured co-chaperone ERp57 by flow cytometry and found that after treatment with **1** for 24 hours, ERp57 increased on the cell surface to a similar extent as did CRT, approximately six-fold (Figure 3.5B). These results are consistent with previous reports that the translocation of these ER-resident chaperones to the plasma membrane occurs by anterograde ER-Golgi transport. [45]

Anthracyclin-induced CRT has previously been reported to be mediated by a caspase 8- and caspase 3/7-dependent pathway that can be disrupted with the pan-caspase inhibitor Z-VAD-fmk (**Z**).[45] Upon co-dosing polyamide **1** with **Z**, however, we saw no decrease in CRT exposure (Figure 3.5C). This caspase-independence was unexpected in light of literature precedent as well as the cytotoxicity we observed of **1** during flow cytometry experiments. We confirmed the lack of PARP cleavage, a caspase substrate cleaved during apoptosis, by immunoblot (Figure 3.5D). We then directly measured caspase activity with a luciferase assay after treatment with hairpin polyamides **1** and **2** as well as **Eto** and **Dox**. We measured a slight increase, approximately 1.2-fold, upon treatment with **1** for 24 hours and no increase after treatment with **2**. In contrast, we measured significant increases of approximately 15-fold each after treatment with **Eto** and **Dox** (Figure 3.6A). The lack of caspase-dependence and caspase activation would suggest the trigger of CRT by **1** is different from anthracyclin DNA intercalators.

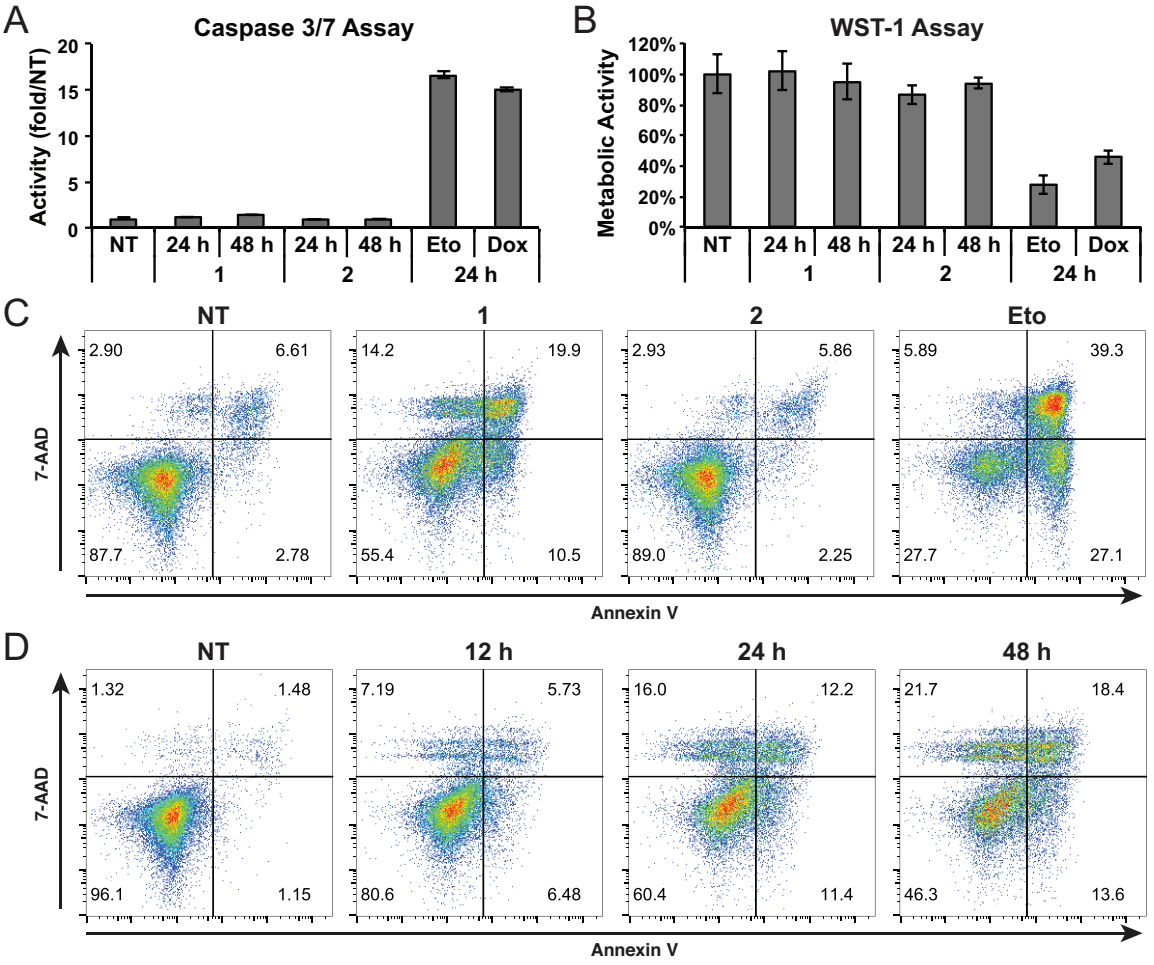

Figure 3.6 Raji cells undergo a slow, necrotic type cell death after treatment with polyamide **1**. A) Caspase 3/7 activity was assessed by a luciferase assay after the indicated treatment. Measurement is representative of two independent experiments and error bars show standard deviations of triplicate measurement. B) Cellular metabolism as a proxy for cytotoxicity was measured with a WST-1 assay. Cytotoxic controls etoposide (**Eto**, 30 μM) and doxorubicin (**Dox**, 5 μM) were included. Measurements were normalized to non-treatment. Graph is representative of two independent experiments and error bars represent standard deviations of technical quadruplicate. C) Flow cytometry assessment of Raji cells treated with the indicated compounds for 24 hours and stained for plasma membrane permeability (7-AAD) and phosphatidylserine exposure (Annexin V). Live: lower left; Early necrotic: upper left; Secondary necrotic: upper right; Apoptotic: lower right. Representative plots shown of triplicate measurement from two independent experiments. D) Assessment as in (B) after 12, 24, and 48 hour exposure to polyamide **1** at 25 μM. Error bars represent standard deviation of triplicate measurement of two independent experiments.

Polyamide 1 induces a slow necrotic-type cell death

We measured cytotoxicity via the metabolic rate with the WST-1 reagent in a colorimetric assay. We were surprised to find that treatment with **1**, at both 24 and 48 hours, had little effect on the bioreduction of WST-1 to the formazan dye, suggesting no diminution of metabolic rate (Figure 3.6B). This is in stark contrast to the cytotoxic **Eto** and **Dox**, which showed drastic reduction in cellular metabolism consistent with the apoptotic program. This led us to assess whether polyamide **1** may direct the Raji cells towards programmed necrosis. Necrosis is an immunogenic, inflammatory type of cell death that is usually attributed to harsh physical insult such as freeze-thaw cycles. Recently, a biologically-controlled necrosis program has been described where cells undergo early plasma membrane permeabilization with active inflammatory signaling and an oxidative burst.[47] We compared the mode of cell death after 24 hour treatment with hairpins **1** and **2**, or **Eto** by flow cytometry. We analyzed plasma membrane permeability and phosphatidylserine exposure on the cell surface to determine subpopulations of live, necrotic, and apoptotic cells after compound exposure. Plasma membrane permeability was assessed through 7-AAD dye exclusion and phosphatidylserine was visualized by dye-conjugated annexin V binding. We found that the non-treated control and treatment with hairpin **2** at 24 hours resulted in little cell death, but treatment with **1** or **Eto** caused significant cell death (Figure 3.6C). Remarkably, there was a distinct and substantial population of cells treated with **1** that lost plasma membrane integrity without phosphatidylserine exposure, indicative of a

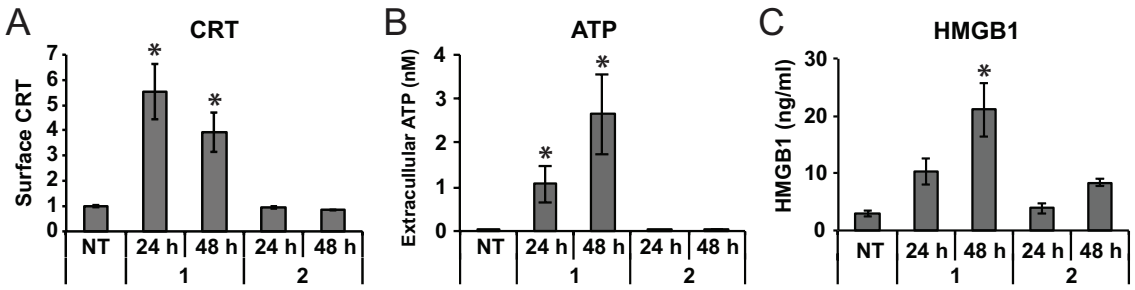

Figure 3.7 Immunogenic signaling is triggered by polyamide **1** treatment. A) CRT was measured by flow cytometry after 24 and 48 h treatment with **1** or **2** at 25 μM. B) Extracellular ATP was measured by a bioluminescence assay after the same treatment. C) HMGB1 in the supernatant was measured by ELISA after treatment with **1** or **2** at 25 μM. CRT flow cytometry and HMGB1 ELISA were measured in triplicate from at least two independent experiments. ATP was measured in quadruplicate in three independent experiments. Error bars are standard deviations and statistically significant increases (two tailed Student's t-test, $p<0.05$) compared to non-treatment are indicated by an asterisk.

necrotic cell death. We observed a continuous population from the upper left to the upper right quadrant in cells treated with polyamide **1**, suggestive of progressive phosphatidylserine exposure in permeabilized cells. The upper right quadrant in all treatment conditions is secondary necrosis, as there are no phagocytes to remove apoptotic or necrotic bodies. There are nearly no cells in the etoposide-treated condition that lie in the upper left quadrant, reflective of a canonical apoptotic cell death with intact membranes displaying phosphatidylserine. The anthracyclins could not be used in this assay due to their inherent fluorescence. We further did a time course of the necrotic effect of polyamide **1** at 12, 24, and 48 hours and found that the cells began permeabilization as early as 12 hours, and underwent further necrosis by 48 hours (Figure 3.6D). These assays together suggest polyamide **1** preferentially tracks Raji cells towards a slow, necrotic-type cell death even though the cells are capable of apoptosis.

Polyamide 1 triggers the release of DAMPs

The inflammatory nature of necrotic cell death can be attributed in part to the release of immune-activating DAMPs.[47,48] We measured levels of CRT, ATP, and HMGB1 after polyamide **1** treatment, as these DAMPs have been described as key factors in a spatiotemporal code of immunogenicity.[13,14] We included polyamide **2** as an in-class control because **2** has been extensively studied in other cancer models.[33] We measured CRT by flow cytometry after 24 and 48 hours of compound exposure at 25 μM and observed a decreasing trend for surface CRT (Figure 3.7A), consistent with reports that CRT is an early response signal.[14] Even at the 25 μM concentration of polyamide **2**, we detected no increase of CRT after 24 hour treatment. Extracellullar ATP was measured with a bioluminescence assay of the supernatant after the same treatment regime (Figure 3.7B). The ATP detected in the media after treatment with hairpin **1** was greatly increased over the non-treated condition. We next analyzed the release of HMGB1 by running a sandwich ELISA for HMGB1 in the supernatant. After treatment for 24 or 48 hours with **1**, a significant increase in excreted HMGB1 was detected in the media (Figure 3.7C). The polyamide **1**-mediated release of CRT, ATP, and HMGB1 in this temporal pattern is consistent with immunogenic signaling described in the literature.

Polyamide 1 treated Raji cells are subject to phagocytosis

Necrotic cell death with an abundance of externalized CRT and other released immunogenic DAMPs should increase phagocytosis. We obtained human peripheral blood macrophages and incubated them for 2.5 hours with Raji cells treated with **1** or **2** at

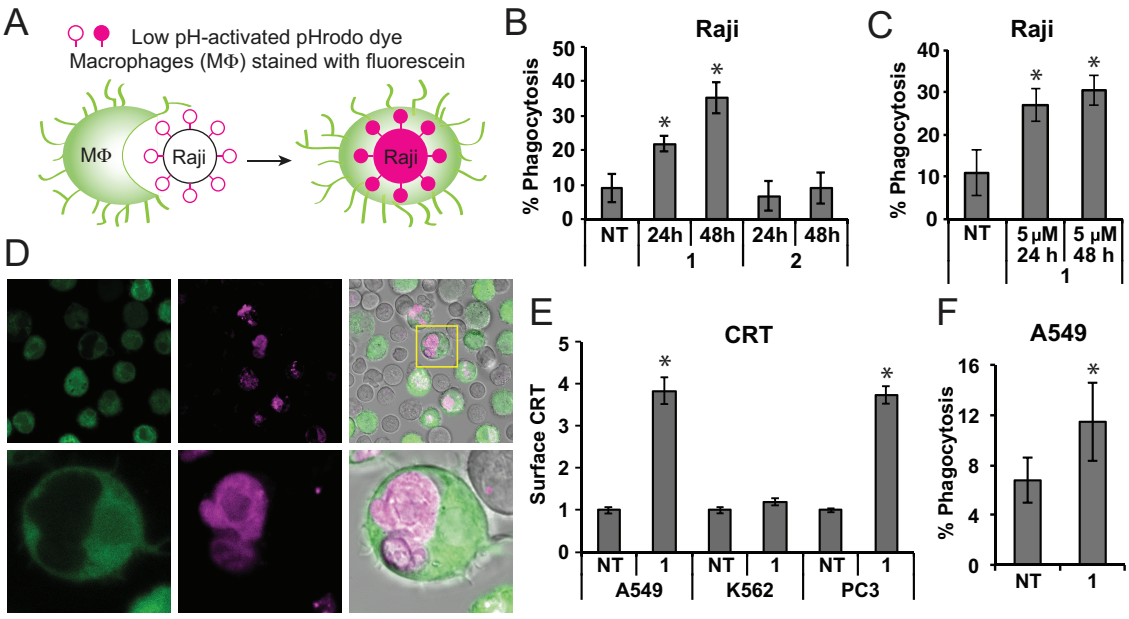

Figure 3.8 Treatment of cells with **1** increases phagocytosis by human macrophages. A) Schematic diagram of fluorescence-revealed phagocytosis using the pH-sensitive pHrodo dye. B) Raji cells treated with the indicated compound at 25 µM for 24 or 48 hours were incubated with human macrophages for 2.5 hours. Fluorescein+ cells were assessed by flow cytometry for double-positive cells to determine % phagocytosis. C) Raji cells were treated with a lower dose of 5 µM of **1** for 24 and 48 hours and assessed for phagocytosis by macrophages in the same manner as in (B). D) Fluorescent images of cells prepared as in B) are shown. Human macrophages are marked green, free Raji cells are grey in the brightfield composite image, and magenta-colored bodies inside macrophages are phagocytosed Raji cells. Yellow box in top row is magnified in bottom row images. E) The cell lines A549, K562, and PC3 were treated with polyamide **1** for 24 hours and screened by flow cytometry for surface CRT. Measurements were in technical triplicate. F) A549 lung carcinoma cells treated with **1** for 24 hours was subjected to human macrophages as described above. Graphs show mean and standard deviation from three independent experiments for (B), (C), (E), and (F). Asterisks indicate statistically significant increases (Student's two tailed t-test, $p<0.05$) compared to the non-treated condition. Images in (d) are representative of two independent experiments.

25 µM for 24 or 48 hours. The Raji cells' plasma membrane was covalently decorated with a pH-sensitive dye (pHrodo) that is activated when engulfed. Macrophages were marked with a cell-permeable fluorescein dye (Figure 3.8A). Macrophages that phagocytosed Raji cells are double positive for fluorescein and activated pHrodo dye. In each experiment, 1000 macrophages were analyzed by flow cytometry per condition. Compared to non-treatment, we found that a greater percentage of macrophages

incubated with polyamide **1**-treated Raji cells were double positive, and more so at 48 than 24 hours (Figure 3.8B). We saw little change when macrophages were incubated with cells treated with **2**. This indicates macrophages phagocytosed Raji cells more efficiently after treatment with polyamide **1**. We also tested the lower concentration of 5 μM of **1** used in the library screening assay, anticipating that immunogenicity may be a threshold effect and that 5 μM may be a more reasonable *in vivo* concentration. We found that the treatment of Raji cells with this lower concentration still increased the percentage of phagocytosis by macrophages (Figure 3.8C). We then verified the phagocytosis assay results with confocal microscopy to ensure that Raji cells were indeed phagocytosed rather than externally adherent (Figure 3.8D). The images show that a fraction of macrophages have internalized Raji cells, which fluoresce with the activated pHrodo dye. The brightfield composite image shows free Raji cells in grey, which are not engulfed by macrophages and lack a robust pHrodo signal. The bottom row shows a magnification of a macrophage after phagocytosis of a large Raji cell body.

Polyamide 1 triggers CRT and phagocytosis in other cancer cell lines

We next explored whether this effect might be specific to the Raji B cell lymphoma model or more general in other cancer cell lines. We screened the A549 lung adenocarcinoma cell line, K562 B cell leukemia cell line, and the PC3 prostate cancer cell line for CRT translocation after treatment with **1**. We observed approximately four-fold increase in CRT surface expression in the A549 and PC3 cell lines (Figure 3.8E). Surprisingly, we did not observe an increase in the K562 B cell leukemia cell line (Figure 3.8E) though they are closest in lineage with the Raji B cells. We then tested the A549

cell line in the phagocytosis assay after 24 hour treatment with 25 μM polyamide **1**. Even though the adherent A549 cell line presents a more difficult target for macrophages, as compared to non-adherent Raji cells, we measured an observable increase in A549 phagocytosis after treatment with polyamide **1** (Figure 3.8F). These results show the effects of polyamide **1** extend beyond the Raji cell line to cells of different lineages but are not completely general.

RNA-seq of Raji cells after treatment with polyamide 1 or 2

To better understand these effects in Raji cells, we examined the change in global gene expression after treatment with the polyamides for 24 hours. We isolated RNA from Raji cells treated with either polyamide **1** or **2**, or untreated and sequenced the transcriptome by next-generation sequencing.[49] The sequenced reads were mapped by Bowtie and Tophat to the Ensembl genes of human genome build 19.[50,51] The non-treated, polyamide **1**-treated, and polyamide **2**-treated samples were done in biological triplicate. The nine total datasets were input into the Cuffdiff algorithm, which identifies differentially expressed genes between datasets, accounting for replicates.[52]

In the polyamide **1**-treated samples, a total of 576 differentially regulated Ensembl genes were identified, of which 528 mapped to unique HGNC genes due to the inclusion of haplotypes in Ensembl. Of these, 236 genes were measured to be significantly upregulated, of which 154 were upregulated by 25% or greater from the non-treated condition (Table 3.1). There were 292 unique HGNC genes downregulated by polyamide **1**, where 64 were changed by more 25% or greater (Table 3.1). A smaller

Table 3.1 Summary of significant, differentially regulated genes from Cuffdiff analysis of RNA-Seq data.

		Ensembl	Unique HGNC Gene	Unique 25% change
Polyamide **1**	Upregulated	278	236	154
	Downregulated	298	292	64
Polyamide **2**	Upregulated	122	121	21
	Downregulated	118	118	47

set of genes were changed by polyamide **2** treatment, with 240 total Ensembl gene expression changes found significant, which mapped to 239 unique HGNC genes (Table 3.1). Of these, 121 genes were upregulated, of which 21 were upregulated by 25% or greater. Of 118 genes downregulated by polyamide **2**, 47 were downregulated by 25% or greater (Table 3.1). A full list of genes up- or down- regulated by 25% or greater upon polyamide **1** or **2** treatment is in Tables 3.2-3.5 at the end of the chapter.

There were several genes of note upregulated upon treatment with polyamide **1**. The gene for tumor necrosis factor (TNF), a major cytokine that regulates inflammation, was upregulated two-fold (Table 3.2).[53] Additionally, the genes HLA-DMA, HLA-DMB, HLA-DRB, and HLA-DQB, which encode the major histocompatibility complex (MHC) class II and accessory factors, were found to be increased ~40-50% (Table 3.2). HLA-E, which codes a non-classical MHC class I molecule that is a ligand for a natural killer cell receptor, was also found to be increased over 40%.[54] The MHC molecules are critical components of antigen recognition in the immune system as they present peptides to T cells in the context of a molecular structure unique to the individual.[55,56] The upregulation

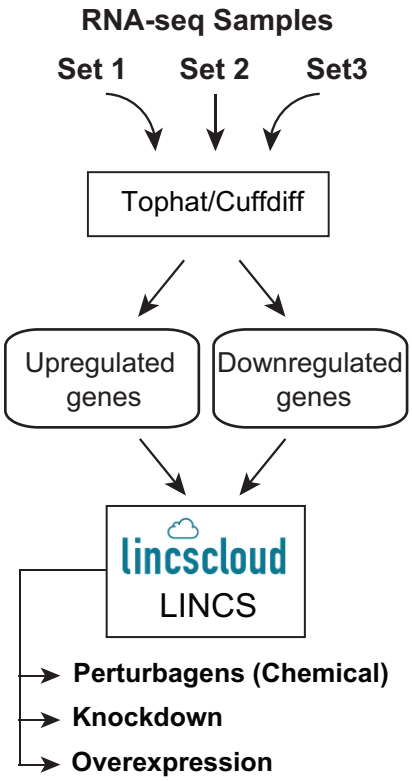

Figure 3.9 Scheme of RNA-Seq analysis pipeline.

of these genes is consistent with the inflammatory signaling observed in the previous assays. The intermediate early genes EGR1, EGR2, EGR4, and FOS are strongly upregulated as well, but given the wide scope of their effects in development, differentiation, and cell death, their role in this case is less clear.[57-59] These genes are markedly absent from the list of genes modulated by polyamide **2**, suggesting that this is not a class effect, but unique to hairpin polyamide **1**.

Genes found to significantly differ from the non-treated condition were then submitted for analysis by a cloud-based program created by the Library of Integrated Network-based Cellular Signatures (LINCS) to compare gene signatures with those in its

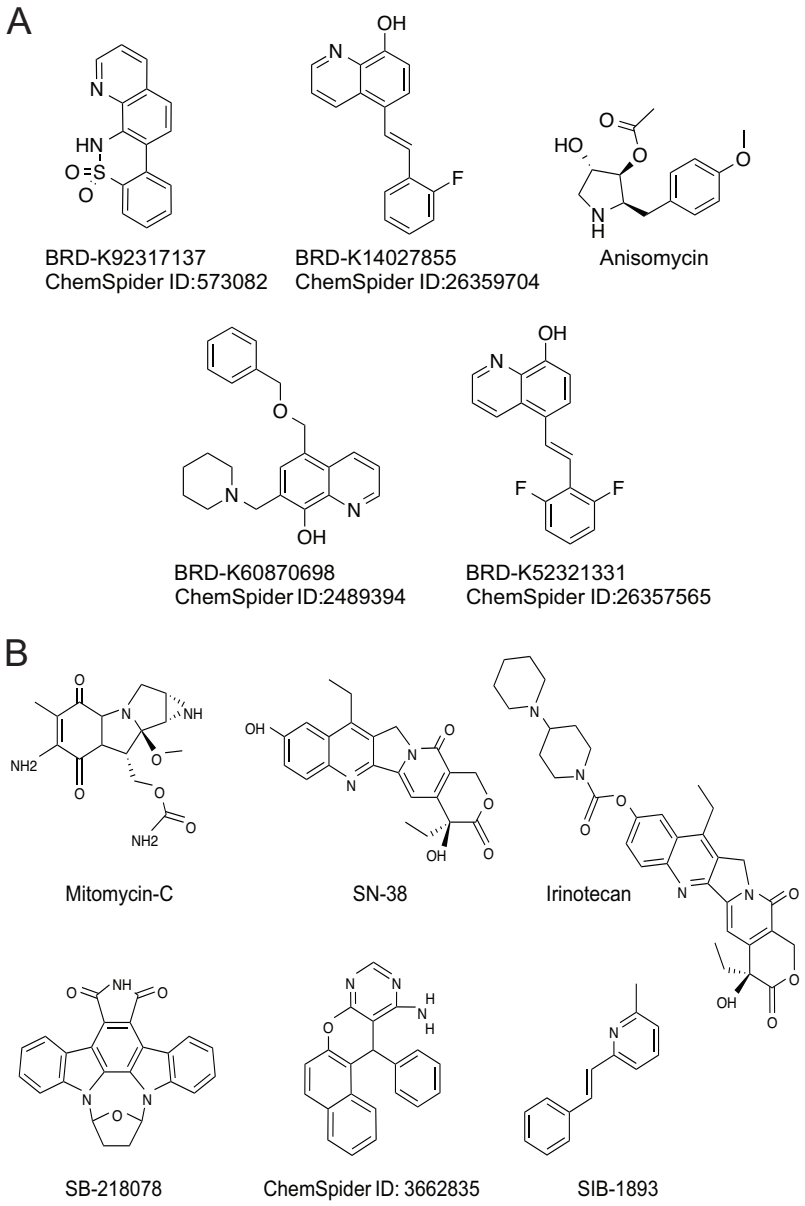

Figure 3.10 Structures of compounds identified by LINCS to have gene expression profiles similar to A) polyamide **1** and B) polyamide **2**.

database of human cells treated with chemical or genetic agents (Figure 3.9).[60] The structures of the top chemical hits in the LINCS analysis for polyamide **1**, shown in Figure 3.10A, are not well studied compounds and were not very informative. In contrast, several cytotoxic DNA binding molecules were identified for polyamide **2**, including the topoisomerase inhibitor irinotecan and its active metabolite SN-38 (Figure 3.10B). This is

in agreement with previous analyses of polyamide **2** in the LREX and VCaP prostate cancer cell lines (Yang, Nickols, Dervan; unpublished) and highlights the differences in biological activity between these two molecules.

The LINCS algorithm also compares the up- and down- regulated gene expression profile with experiments where single genes were overexpressed. The top "overexpression" signatures identified by LINCS included genes that encode MAP2K6, GADD45A, TIRAP, and interferon-β. MAP2K6 is a TNF-responsive kinase of p38 MAPK that integrates stress signals and cytokine signaling.[61] GADD45A is a member of a family of stress sensors that is responsive to genotoxic stress and affects cell cycling, DNA repair, and cell death.[62] TIRAP is a signal transducing molecule for the TLR2 and TLR4 receptors, which activate the innate immune response.[63] Interferon-β is a cytokine often produced in response to viral infection that primes adaptive immunity.[64] These expression signatures include aspects of immune activation and cellular or genotoxic stress signaling and may provide leads towards understanding the mechanism of polyamide **1** activity.

3.3 Discussion

In this study, we have discovered a Py-Im polyamide capable of triggering the release of immunogenic signals in a necrotic-type cell death. Treatment with polyamide **1** increased the externalization of CRT, HMGB1, and ATP, which have been characterized to be key signals of immunogenicity. We further observed that polyamide **1** causes permeabilization of the plasma membrane in a subpopulation of treated Raji cells, which

grows from 12 to 48 hours. This occurs even as the apoptotic cell death pathway remains competent, as demonstrated by the distribution profile observed after **Eto** treatment of Raji cells. We conclude that polyamide **1** preferentially triggers a necrotic-type, likely highly immunogenic cell death, an effect we are not aware has precedent with a small molecule synthetic ligand.

Phagocytosis by antigen-presenting cells is a critical step in a chain of events towards leveraging the specificity and power of the immune system towards attacking the offending target. We saw increased phagocytosis of polyamide **1**- treated cells by macrophages, as would be expected upon the death of Raji cells with externalized pro-phagocytic CRT. The observed phagocytosis and inflammatory DAMPs released into the tumor microenvironment makes plausible that the immune system would become primed towards antigens of Raji cells. Reports have shown engulfment by macrophages can activate an effective anti-cancer T cell response.[11] The application of polyamide **1** on cancer in the context of a full immune system remains to be explored.

That the DNA sequence preference of **1** is identical with that of human telomeres was indicated by the pairing rules and confirmed by Bind-n-Seq. Whether the mechanism of action for polyamide **1** is through its sequence-specific DNA binding capacity remains an open question. Though polyamides have generally been characterized to act in a DNA-binding mode, we cannot exclude that polyamide **1** may act as an aptamer binding to unknown target proteins. The translocation of CRT after polyamide **1** treatment was observed in multiple, though not all, cell lines and suggests there is a conserved pathway

that leads to this phenotype that is retained in many cancer cell lines. The RNA-Seq analysis showed that polyamide **1** triggered the expression of immune activating molecules. LINCS analysis of the transcriptomic data suggests similarity to several stress response and immune activating gene patterns. We expect the elucidation of the mechanism of action will reveal important signaling networks involved in immunosurveillance of cancer cells.

Conclusion

The effects of polyamide **1** are compelling because immunogenic cancer cell death is cleared in the natural setting and thus difficult to observe. Further study may reveal tumor suppressive signaling pathways that can be exploited to extrinsically control cancer even as cell-intrinsic mechanisms fail. The failure of anthracyclins to elicit CRT in Raji cells when they have previously been shown to be effective in CT26 murine colon cancer cells [9] underscores the heterogeneity of cancers. As cancers have heterogeneous mechanisms for evading elimination by the immune system, a corresponding diversity of immunogenicity agents will be important for both shedding light on new biology and developing immuno-oncologic therapies.

3.4 Materials and methods

Chemicals and Reagents. All chemicals were purchased from Sigma-Adlrich unless otherwise noted. Py-Im polyamides were synthesized by microwave-assisted, solid-phase synthesis on Kaiser oxime resin (Novabiochem) according to previously

Table 3.6. Mass spectrometry (MALDI-TOF) for Py-Im polyamides.

Polyamide	**Molecular formula**	**[Mass + H]**	**Found Mass**
ImImImPy-(R)$^{\alpha\text{-}NH2}$γ-PyPyPyPy-(+)-IPA (**1**)	$C_{64}H_{76}N_{23}O_{12}^{+}$	1358.6	1358.5
ImPyPyPy-(R)$^{\alpha\text{-}NH2}$γ-ImPyPyPy-(+)-IPA (**2**)	$C_{65}H_{77}N_{22}O_{12}^{+}$	1357.6	1357.1
ImImPyPy-(R)$^{\alpha\text{-}NH2}$γ-ImPyPyPy-(+)-IPA (**3**)	$C_{64}H_{76}N_{23}O_{12}^{+}$	1358.6	1358.0
CtPyPyIm-(R)$^{\alpha\text{-}NH2}$γ-PyImPyPy-(+)-IPA (**4**)	$C_{64}H_{73}ClN_{21}O_{12}S^{+}$	1394.5	1394.1
PyImPyIm-(R)$^{\alpha\text{-}NH2}$γ-PyImβIm-(+)-IPA (**5**)	$C_{60}H_{74}N_{23}O_{12}^{+}$	1308.6	1309.0
ImImIm-(+)-IPA (**6**)	$C_{30}H_{38}N_{11}O_{6}^{+}$	648.3	648.8
ImImImPy-(R)$^{\alpha\text{-}NH2}$γ-PyPyPyPy-(+)-4PEG-Biotin (**1b**)	$C_{77}H_{107}N_{26}O_{16}S^{+}$	1683.8	1683.1

described protocols. [65,66] Polyamide **5** was synthesized on hydrazine resin (855037, Novabiochem) in the same manner as the other polyamides and cleaved from resin in the same manner after 10 minute oxidation of the hydrazine by Cu(II)SO_4 in pyridine and DMF. Polyamides were purified by reverse-phase HPLC and lyophilized. EZ-Link NHS-PEG4-biotin (Pierce) was conjugated in 5% Hünig's base in DMF. Purity and identity of compounds were verified by analytical HPLC and matrix-assisted laser desorption/ionization time-of-flight (MALDI-TOF) mass spectrometry (Table 3.6).

Brefeldin A was purchased from BD biosciences, 7-AAD from eBiosciences), and Z-VAD-fmk from Promega. Antibodies purchased from Abcam are: polyclonal rabbit anti-calreticulin (ab2907), polyclonal rabbit anti-ERp57 (ab10287), and polyclonal goat anti-rabbit Alexa Fluor 488 (ab150081). Antibodies from Life Technologies are: anti-Annexin

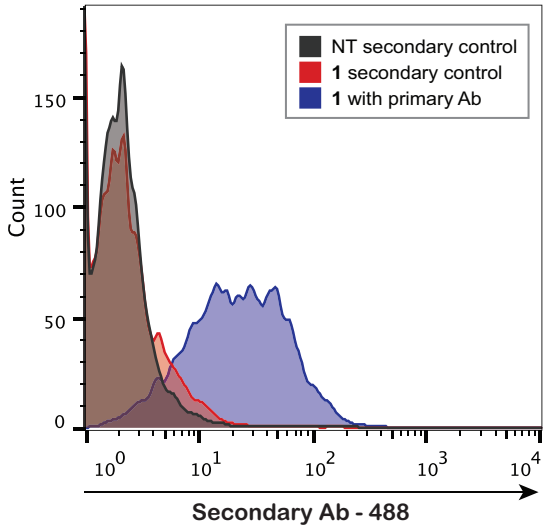

Figure 3.11 Specificity control for CRT primary antibody.

V Alexa Fluor 488 conjugate (A13201) and mouse monoclonal anti-actin (AM4302). Antibodies from Cell Signaling Technologies are: rabbit polyclonal anti-PARP (9542) and rabbit monoclonal anti-phospho-H2AX (ser139, 9718).

Cell culture. Raji cells (ATCC) were maintained in RPMI media (Life Technologies) with 10% fetal bovine serum (Omega Scientific) and 5mM glutamine (Life Technologies). K562 cells (ATCC) were cultured in IMDM (ATCC) media and 10% FBS. A549 and PC3 cells (ATCC) were maintained in Kaign's modified F-12K media (Gibco) supplemented with 10% FBS and 5 mM glutamine. Peripheral blood macrophages (Stemcell Technologies) were thawed and plated in DMEM (ATCC) and supplemented with 5 mM glutamine and 10% FBS for at least two days and no longer than six days before use.

Flow cytometry. Raji and K562 cells were plated at 1×10^5 cells/ml in 96-well plates at 100 µl and treated immediately after plating. A549 and PC3 cells were plated in

Table 3.7. Cell death flow cytometry after different treatments for 24 hours.

	Live	Necrotic	Apoptotic	2º Necrotic
NT	86.9 (±1.6)	2.0 (±0.4)	5.8 (±1.3)	5.3 (±0.3)
1	57.0 (±2.2)	11.9 (±1.1)	12.8 (±1.2)	18.4 (±1.2)
2	88.1 (±1.0)	2.3 (±0.3)	5.2 (±0.9)	4.5 (±0.2)
Eto	26.7 (±0.7)	5.3 (±0.2)	32.7 (±1.1)	35.3 (±1.0)

Table 3.8. Timecourse of cell death flow cytometry after treatment with **1**.

	Live	Necrotic	Apoptotic	2º Necrotic
NT	95.7 (±0.5)	1.7 (±0.4)	1.1 (±0.1)	1.5 (±0.1)
12 h	47.5 (±1.1)	19.6 (±2.0)	14.4 (±1.1)	18.5 (±0.5)
24 h	59.7 (±4.8)	15.6 (±1.0)	11.8 (±1.0)	12.9 (±3.0)
48 h	79.4 (±1.5)	7.7 (±1.1)	6.7 (±0.3)	6.2 (±0.4)

24-well plates at 6×10^4 cells/ml at 400 µl and were allowed to adhere overnight prior to treatment. Adherent cells were harvested with Accutase (Life Technologies).

For the CRT and ERp57 detection experiments, harvested cells were washed with cold staining buffer: HBSS (Life Technologies) with 2.5mg/ml BSA (Amresco), 10mM HEPES (Life Technologies), 0.1 mM $MgCl_2$ (Life Technologies), and DNAse (Roche). Cells were incubated with human FcR block (eBiosciences) and primary antibody in cold staining buffer. This was followed by washing and incubation with dye-conjugated anti-rabbit secondary antibody. 7-AAD, forward- and side- scatter were used to gate for live cells. Secondary antibody alone was used as a control (Figure 3.11). The median

Table 3.9 Table of top motifs and associated e-values for three Bind-n-Seq analyses of biotin-conjugate polyamide **1b**.

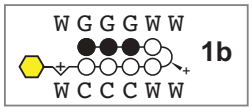

Concentration	Primary motif	E-value	Secondary motif	E-value
250 nM		2.6e-5582		4.5e-207
25 nM		7.3e-509		1.1e-028
25 nM		3.9e-129		9.1e-008

fluorescence intensity of live cells is normalized to non-treatment. Data was acquired on the FACS Calibur and analyzed with Flowjo software. Measurements and standard deviations are in triplicate and representative of at least two independent experiments; asterisk indicates $p<0.05$ by two-tailed Student's t-test compared to non-treatment.

For cell death analysis flow cytometry experiments, Raji cells were harvested after treatment and washed with cold staining buffer and incubated with FcR block and dye-conjugated anti-Annexin V. Cells were washed with staining buffer and taken for immediate analysis. 7-AAD was added to samples maintained at 4 ºC and data was acquired soon thereafter on the MACS VYB. Data was acquired in triplicate from two independent experiments and analyzed with Flowjo (Table 3.7 and 3.8).

Bind-n-Seq of polyamide 1b. Highest affinity DNA binding sites of polyamide-biotin conjugate **1b** were determined according to previously reported methods. [43] In brief, polyamide **1b** was equilibrated at 25 or 250 nM overnight in a DNA library of all possible 21mers. DNA bound to **1b** was affinity purified with streptavidin magnetic beads (M-280 Dynabeads, Life Technologies) and eluted. Isolated DNA was amplified by touchdown PCR and submitted for sequencing on an Illumina HiSeq 2000 Genome Analyzer. The MERMADE script was used to distribute data by barcode and a fasta file of a random 25% of sequences was generated for DREME motif analysis. Data is representative of three independent experiments (Table 3.9).

DNA thermal denaturation assay. DNA of the sequence 5'-CTTAGGGTTAGC-3' and its complement were purchased from Integrated DNA Technologies and annealed. The oligonucleotides were mixed with hairpin polyamide **1** to a final concentration of 2 and 3 μM, respectively, in 1 mL total volume. An aqueous solution of 10 mM sodium cacodylate, 10 mM KCl, 10 mM MgCl2, and 5 mM CaCl2 at pH 7.0 was used as analysis buffer. The assay utilized a Varian Cary 100 spectrophotometer to heat samples to 90 °C, cool to a starting temperature of 25 °C, and then heat at a rate of 0.5 °C/min to 90 °C. Denaturation profiles were recorded at $\lambda = 260$ nm and melting temperatures were detected by the maximum of the first derivative. Data shows the combined mean and standard deviation of triplicate measurements from two independent experiments.

Immunoblot assays. Raji cells were plated at 10^5 cells/ml in 10 cm diameter dishes and dosed with the indicated treatment. Cells were washed with cold PBS and lysed for ten minutes in lysis buffer (50 mM Tris-HCl pH 7.4, 1 mM EDTA, 150 mM

NaCl, 1% Triton X-100) containing protease inhibitors (Complete, Roche), 1 mM PMSF, and phosphatase inhibitors. Samples were clarified by centrifugation at 14,000 × g for ten minutes, quantified with the Bradford reagent (Bio-rad), denatured by boiling in Laemmli buffer (LI-COR) for 5 min, and separated by sodium dodecyl sulphate-polyacrylamide gel electrophoresis using AnyKD gradient gels (Biorad). Protein was transferred to a PVDF membrane (Millipore) and blocked with Odyssey blocking buffer (LI-COR). Both primary antibodies and appropriate IR-dye conjugated secondary antibodies (LI-COR) were incubated in blocking buffer with 0.2% Tween. Anti-actin was used to control for equal loading and experiments were done in at least two independent biological replicates. Bands were visualized on a LI-COR Odyssey infrared imager.

ATP bioluminescence assay. Raji cells were plated into 96-well cell culture plates at 200 µl per well and 10^5 cells/ml, in quadruplicate per condition. After the indicated treatment, media and cells were transferred to a 96-well PCR plate and centrifuged at 130 × g for 5 minutes. The supernatant was collected for analysis of ATP content using an ATP bioluminescence kit (FLAA, Sigma). The assay was performed according to the manufacturer's protocol and luminescence was measured using a Flexstation 3. Measurements and standard deviation are technical quadruplicate and biological triplicate. Asterisk indicates $p<0.05$ by two-tailed Student's t-test compared to non-treatment.

HMGB1 ELISA. Raji cells were plated into 96-well cell culture plates at 100 µl per well, 10^5 cells/ml, in duplicate. Cells were treated with polyamide **1** and **2** as indicated and the supernatant collected. HMGB1 was measured using the Shino-Test ELISA kit (IBL international) according to the manufacturer's instructions on the

Flexstation 3. Measurement and standard deviations were determined from technical duplicate from two independent replicates.

Caspase luciferase assay. Raji cells were plated into 96-well cell culture plates at 100 µl per well and 10^5 cells/ml, in triplicate per condition. Media was included as a blank control. After the indicated treatment, media and cells were transferred to an opaque white 96-well plate containing 100 µl in each well of the caspase-dependent luciferase reagent, prepared per the manufacturer's instructions (Caspase-Glo 3/7, Promega). The mixture was left at room temperature for 1 hour prior to measurement on the Flexstation 3 (Molecular Devices). Measurements and standard deviations were determined in triplicate and done in biological duplicate.

Metabolic activity assay. Raji cells were plated into 96-well clear bottom cell culture plates at 100 µl per well and 10^5 cells/ml, in triplicate per indicated condition. Media was used as a background control. Metabolic activity was assessed using the WST-1 reagent (Roche) per the manufacturer's instructions. Measurements and standard deviations were determined in triplicate and done in biological duplicate.

Phagocytosis assay. Peripheral blood macrophages were plated at 2×10^4 cells per well in 24 or 48-well plates in DMEM. Immediately prior to use, macrophages were washed with HBSS and stained with carboxyfluorescein diacetate succinimidyl ester (CFSE, eBioscience) in HBSS for 5 min. Macrophages were washed of excess dye and returned to DMEM for incubation. Target Raji cells were plated in 96-well plates at 1×10^5 cells/ml in 200 µl of RPMI and treated as described. Target A549 cells were plated in 24-well plates at 2×10^4 cells per well 15 hours before beginning treatment. After treatment, cells were harvested with Accutase if necessary and washed with HBSS and

incubated with pHrodo succinimidyl ester (Life Technologies) diluted to 2 μM in HBSS for 5 min. Cells were then washed by centrifugation at 150 × g, re-suspended in DMEM, counted on a Biorad TC10 cell counter, and 5×10^4 cells per well were added to macrophages. After incubation for 2.5 hours at 37 ºC, media and non-adherent cells in each sample were aspirated and saved. Adherent cells were trypsinized, aspirated, and combined with saved media mixture. Cells were washed once with PBS and fixed in 1% formaldehyde and kept at 4 ºC until assessment on the MACS VYB flow cytometer. The percentage of phagocytosis was calculated as the percentage of double positive cells among fluorescein+ macrophages. Measurements and standard deviations are taken from three independent experiments, and asterisks indicate $p<0.05$ by two-tailed Student's t-test compared to non-treatment.

Confocal microscopy. For images of phagocytosis, cells treated in the manner described above were put on 35 mm glass-bottom dishes (MatTek). Confocal images were acquired using a 40× oil immersion objective on a Zeiss LSM 5 Exciter microscope.

RNA-Seq. Raji cells were plated in two 175 cm^2 flasks per condition at 4×10^5 cells per ml with 20 ml of RPMI in each flask. Non-treatment, 25 μM polyamide **1**-, and 25 μM polyamide **2**- treatment was prepared at the same time. After 24 hours incubation, cells were washed with PBS twice by centrifugation and pelleted in a 15 ml falcon tube. The cells were suspended in Trizol and lysed by repeated extrusion from a syringe needle and vortexing. The samples were frozen and stored in a -80 ºC freezer, until three biological replicates were collected. The Trizol solution was thawed and RNA was isolated from Trizol (Life Technologies), and precipitated with linear acrylamide (Life Technologies). The RNA was washed and subjected to DNase treatment (Roche) prior to

quantitation. Samples each containing 10 μg of RNA in 100 μl of TE buffer was submitted for sequencing to the Millard and Muriel Jacobs Genetics and Genomics Laboratory on the Illumina Genome Analyzer.

3.5 Acknowledgments

This work was supported by the National Institutes of Health Grant GM51747 and Tobacco-Related Disease Research Program (award number 20DT-0037 to J.S.K., dissertation research award). We thank Rochelle Diamond and Diana Perez of the Caltech Flow Cytometry Cell Sorting Facility for help with flow cytometry. Sequencing was conducted with the help of Dr. Igor Antoshechkin at the Millard and Muriel Jacobs Genetics and Genomics Laboratory at the California Institute of Technology; mass spectrometry analyses were performed in the Mass Spectrometry Laboratory of the Division of Chemistry and Chemical Engineering at the California Institute of Technology; gels were scanned in the Center for the Chemistry of Cellular Signaling at the California Institute of Technology.

Table 3.2 Genes upregulated greater than 25% after treatment with polyamide **1** for 24 hours compared to non-treatment.

Ensembl Gene	Gene	Locus	Ratio	NT fpkm	GGGW fpkm	p_val	q_val
ENSG00000122877	EGR2	chr10:64571755-64679660	20.33	0.10	2.09	0.0002	0.0109
ENSG00000120738	EGR1	chr5:137801178-137805004	9.85	3.01	29.67	0.0000	0.0000
ENSG00000170345	FOS	chr14:75745476-75748933	6.90	1.96	13.54	0.0000	0.0006
ENSG00000027869	SH2D2A	chr1:156776034-156851642	5.08	0.40	2.03	0.0001	0.0088
ENSG00000135625	EGR4	chr2:73518057-73520833	4.80	0.18	0.87	0.0000	0.0010
ENSG00000135363	LMO2	chr11:33880121-33913836	4.25	8.12	34.53	0.0000	0.0000
ENSG00000110848	CD69	chr12:9905081-9913497	3.04	2.71	8.24	0.0000	0.0000
ENSG00000185022	MAFF	chr22:38597888-38612518	3.01	1.95	5.89	0.0000	0.0012
ENSG00000111679	PTPN6	chr12:7055630-7070479	3.00	82.60	247.93	0.0000	0.0000
ENSG00000059804	SLC2A3	chr12:7917811-8250367	2.95	4.66	13.74	0.0000	0.0000
ENSG00000127124	HIVEP3	chr1:41972035-42501596	2.70	2.37	6.40	0.0000	0.0000
ENSG00000100985	MMP9	chr20:44637546-44688789	2.55	0.51	1.31	0.0000	0.0032
ENSG00000227039	ITGB2-AS1	chr21:46305867-46351904	2.54	3.55	9.02	0.0008	0.0362
ENSG00000166886	NAB2	chr12:57482676-57607134	2.51	22.08	55.39	0.0000	0.0000
ENSG00000197629	MPEG1	chr11:58938902-58980424	2.47	0.50	1.24	0.0000	0.0000
ENSG00000168209	DDIT4	chr10:74033677-74035794	2.43	72.45	176.07	0.0000	0.0000
ENSG00000228978	TNF	chr6_apd_hap1:2859028-2860831	2.31	1.07	2.46	0.0001	0.0053
ENSG00000204490	TNF	chr6_cox_hap2:3052959-3055729	2.26	1.06	2.39	0.0000	0.0010
ENSG00000206439	TNF	chr6_qbl_hap6:2836981-2839753	2.26	1.06	2.39	0.0000	0.0010
ENSG00000223952	TNF	chr6_mcf_hap5:2923049-2925819	2.26	1.06	2.39	0.0000	0.0010
ENSG00000228321	TNF	chr6_mann_hap4:2886227-2888997	2.26	1.06	2.39	0.0000	0.0010
ENSG00000228849	TNF	chr6_dbb_hap3:2828884-2831654	2.26	1.06	2.39	0.0000	0.0010
ENSG00000230108	TNF	chr6_ssto_hap7:2874144-2876914	2.26	1.06	2.39	0.0000	0.0010
ENSG00000232810	TNF	chr6:31543343-31546113	2.26	1.06	2.39	0.0000	0.0010
ENSG00000118515	SGK1	chr6:134490383-134639250	2.23	23.02	51.38	0.0000	0.0000
ENSG00000138166	DUSP5	chr10:112257595-112271302	2.21	18.34	40.60	0.0000	0.0000
ENSG00000108984	MAP2K6	chr17:67410837-67538451	2.21	2.04	4.50	0.0000	0.0000
ENSG00000247095	MIR210HG	chr11:565659-568457	2.10	12.69	26.61	0.0000	0.0003
ENSG00000161929	SCIMP	chr17:5095378-5151364	2.09	3.69	7.71	0.0000	0.0000
ENSG00000114268	PFKFB4	chr3:48555116-48601206	2.03	11.94	24.26	0.0000	0.0000
ENSG00000158050	DUSP2	chr2:96808904-96811179	1.97	69.35	136.93	0.0000	0.0000

ENSG00000090104	RGS1	chr1:192544856-192549161	1.90	3.88	7.39	0.0000	0.0002
ENSG00000160888	IER2	chr19:13261281-13265716	1.86	51.33	95.61	0.0000	0.0000
ENSG00000226979	LTA	chr6:31539830-31542101	1.82	1.98	3.60	0.0001	0.0070
ENSG00000126860	EVI2A	chr17:29335514-29709134	1.78	6.55	11.66	0.0000	0.0000
ENSG00000128016	ZFP36	chr19:39897486-39900045	1.71	13.43	23.01	0.0000	0.0000
ENSG00000160255	ITGB2	chr21:46305867-46351904	1.70	57.51	97.85	0.0000	0.0000
ENSG00000137101	CD72	chr9:35605366-35647096	1.68	37.22	62.43	0.0000	0.0000
ENSG00000185650	ZFP36L1	chr14:69254376-69263190	1.67	182.58	305.21	0.0000	0.0000
ENSG00000125245	GPR18	chr13:99853027-100038688	1.65	3.75	6.20	0.0002	0.0136
ENSG00000179344	HLA-DQB1	chr6:32627243-32636160	1.65	89.37	147.42	0.0000	0.0000
ENSG00000112137	PHACTR1	chr6:12717892-13328776	1.65	10.17	16.76	0.0002	0.0112
ENSG00000166068	SPRED1	chr15:38544526-38649450	1.64	7.65	12.55	0.0006	0.0270
ENSG00000226397	C12orf77	chr12:25146357-25150453	1.63	8.47	13.81	0.0000	0.0006
ENSG00000111678	C12orf57	chr12:7052140-7055166	1.62	36.86	59.71	0.0000	0.0000
ENSG00000156738	MS4A1	chr11:60223224-60238233	1.61	436.07	701.54	0.0000	0.0000
ENSG00000143851	PTPN7	chr1:202116140-202130716	1.61	44.45	71.43	0.0000	0.0000
ENSG00000154127	UBASH3B	chr11:122526382-122685181	1.60	23.67	37.92	0.0000	0.0004
ENSG00000087074	PPP1R15A	chr19:49375648-49379318	1.60	6.58	10.51	0.0000	0.0000
ENSG00000100290	BIK	chr22:43506753-43525718	1.59	50.13	79.62	0.0000	0.0000
ENSG00000204852	TCTN1	chr12:111051831-111142755	1.56	47.20	73.58	0.0000	0.0001
ENSG00000234883	MIR155HG	chr21:26934220-26947480	1.55	12.54	19.48	0.0000	0.0000
ENSG00000138821	SLC39A8	chr4:103172197-103371167	1.54	70.90	109.02	0.0000	0.0034
ENSG00000198873	GRK5	chr10:120967100-121215131	1.54	8.25	12.69	0.0004	0.0210
ENSG00000122884	P4HA1	chr10:74766974-74856732	1.53	30.26	46.31	0.0000	0.0000
ENSG00000142227	EMP3	chr19:48828628-48833810	1.52	19.49	29.70	0.0000	0.0000
ENSG00000184574	LPAR5	chr12:6728000-6745613	1.51	10.56	15.99	0.0000	0.0000
ENSG00000241674	HLA-DMB	chr6_qbl_hap6:4134532-4181419	1.50	12.75	19.15	0.0004	0.0194
ENSG00000242386	HLA-DMB	chr6_mcf_hap5:4239256-4283840	1.50	11.71	17.57	0.0008	0.0361
ENSG00000239329	HLA-DMB	chr6_mann_hap4:4359616-4406503	1.50	12.85	19.25	0.0004	0.0200
ENSG00000241296	HLA-DMB	chr6_ssto_hap7:4333159-4430060	1.50	11.81	17.66	0.0008	0.0361
ENSG00000196968	FUT11	chr10:75532048-75538821	1.49	23.20	34.68	0.0000	0.0022
ENSG00000109929	SC5D	chr11:121163161-121179403	1.49	52.42	78.34	0.0000	0.0002
ENSG00000086619	ERO1LB	chr1:236305831-236445319	1.49	10.14	15.14	0.0004	0.0202
ENSG00000134061	CD180	chr5:66478102-66492627	1.49	30.00	44.67	0.0000	0.0000
ENSG00000242574	HLA-DMB	chr6:32902405-32949282	1.49	6.62	9.86	0.0008	0.0364

ENSG00000226264	HLA-DMB	chr6_dbb_hap3:4183742-4202240	1.49	13.07	19.42	0.0005	0.0254
ENSG00000206493	HLA-E	chr6_qbl_hap6:1750158-1754897	1.48	15.79	23.41	0.0000	0.0001
ENSG00000229252	HLA-E	chr6_dbb_hap3:1750883-1755622	1.48	15.79	23.41	0.0000	0.0001
ENSG00000233904	HLA-E	chr6_cox_hap2:1969307-1974046	1.48	15.79	23.41	0.0000	0.0001
ENSG00000171223	JUNB	chr19:12902309-12904124	1.48	62.40	92.44	0.0000	0.0000
ENSG00000230254	HLA-E	chr6_ssto_hap7:1789533-1794272	1.48	16.26	24.09	0.0000	0.0000
ENSG00000242092	HLA-DMB	chr6_apd_hap1:4189389-4207888	1.48	13.01	19.22	0.0006	0.0285
ENSG00000122986	HVCN1	chr12:111051831-111142755	1.48	15.71	23.21	0.0002	0.0124
ENSG00000140563	MCTP2	chr15:94774766-95023632	1.47	8.01	11.80	0.0007	0.0334
ENSG00000236632	HLA-E	chr6_mann_hap4:1805321-1810060	1.46	11.29	16.53	0.0000	0.0013
ENSG00000204592	HLA-E	chr6:30457243-30461982	1.46	11.29	16.53	0.0000	0.0013
ENSG00000225201	HLA-E	chr6_mcf_hap5:1839107-1843846	1.46	11.29	16.53	0.0000	0.0013
ENSG00000146386	ABRACL	chr6:139349818-139364439	1.45	55.89	81.21	0.0000	0.0000
ENSG00000136286	MYO1G	chr7:45002260-45018697	1.45	16.13	23.43	0.0000	0.0000
ENSG00000154642	C21orf91	chr21:19135631-19639690	1.44	25.30	36.51	0.0000	0.0000
ENSG00000117394	SLC2A1	chr1:43391518-43424530	1.44	112.09	161.77	0.0000	0.0000
ENSG00000140398	NEIL1	chr15:75639295-75648087	1.44	31.03	44.64	0.0000	0.0019
ENSG00000240409	MTATP8P1	chr1:536815-660287	1.43	526.42	753.97	0.0000	0.0001
ENSG00000198355	PIM3	chr22:50354160-50357728	1.42	93.39	132.75	0.0000	0.0000
ENSG00000196405	EVL	chr14:100437785-100610573	1.42	71.85	101.83	0.0001	0.0064
ENSG00000198502	HLA-DRB5	chr6:32485119-32498064	1.40	21.77	30.50	0.0000	0.0001
ENSG00000239463	HLA-DMA	chr6_mcf_hap5:4239256-4283840	1.40	18.89	26.41	0.0002	0.0092
ENSG00000243215	HLA-DMA	chr6_ssto_hap7:4333159-4430060	1.40	18.93	26.43	0.0002	0.0094
ENSG00000243719	HLA-DMA	chr6_cox_hap2:4346929-4393826	1.40	18.95	26.46	0.0002	0.0096
ENSG00000243189	HLA-DMA	chr6_mann_hap4:4359616-4406503	1.40	18.86	26.33	0.0002	0.0091
ENSG00000242685	HLA-DMA	chr6_qbl_hap6:4134532-4181419	1.40	18.87	26.33	0.0002	0.0091
ENSG00000202198	RN7SK	chr6:52860417-52860748	1.40	83.52	116.54	0.0001	0.0067
ENSG00000168389	MFSD2A	chr1:40420801-40435638	1.40	21.97	30.64	0.0000	0.0001
ENSG00000204257	HLA-DMA	chr6:32902405-32949282	1.39	18.51	25.80	0.0002	0.0116
ENSG00000242361	HLA-DMA	chr6_apd_hap1:4189389-4207888	1.39	26.12	36.34	0.0004	0.0199
ENSG00000196126	HLA-DRB1	chr6:32546545-32557625	1.39	28.09	39.07	0.0000	0.0000
ENSG00000227357	HLA-DRB4	chr6_ssto_hap7:3850430-4111880	1.39	23.95	33.30	0.0000	0.0001
ENSG00000231021	HLA-DRB4	chr6_mcf_hap5:3882320-3897284	1.39	23.94	33.28	0.0000	0.0001
ENSG00000023330	ALAS1	chr3:52232101-52248343	1.39	36.53	50.77	0.0012	0.0495
ENSG00000196101	HLA-DRB3	chr6_qbl_hap6:3720953-3734041	1.39	65.61	91.18	0.0000	0.0000

ENSG00000241394	HLA-DMA	chr6_dbb_hap3:4183742-4202240	1.39	23.65	32.86	0.0007	0.0326
ENSG00000114480	GBE1	chr3:81538849-81811312	1.39	12.41	17.23	0.0000	0.0001
ENSG00000166128	RAB8B	chr15:63481667-63559981	1.39	20.63	28.62	0.0002	0.0117
ENSG00000229074	HLA-DRB1	chr6_mann_hap4:3951045-4028663	1.39	19.23	26.68	0.0000	0.0004
ENSG00000236884	HLA-DRB1	chr6_dbb_hap3:3820127-3854230	1.39	19.88	27.56	0.0000	0.0003
ENSG00000166848	TERF2IP	chr16:75661621-75795051	1.38	77.41	107.14	0.0000	0.0000
ENSG00000196735	HLA-DQA1	chr6:32595955-32614839	1.38	93.11	128.62	0.0000	0.0000
ENSG00000125753	VASP	chr19:46010687-46030236	1.38	52.54	72.51	0.0000	0.0000
ENSG00000206237	HLA-DQB1	chr6_cox_hap2:4064608-4080088	1.38	9.54	13.15	0.0000	0.0027
ENSG00000206302	HLA-DQB1	chr6_qbl_hap6:3851061-3866542	1.38	9.54	13.15	0.0000	0.0027
ENSG00000150347	ARID5B	chr10:63661058-63856703	1.38	4.51	6.21	0.0000	0.0001
ENSG00000132963	POMP	chr13:29233240-29253062	1.38	55.20	75.95	0.0000	0.0000
ENSG00000231679	HLA-DRB3	chr6_cox_hap2:3934114-3947232	1.38	50.41	69.35	0.0000	0.0000
ENSG00000124762	CDKN1A	chr6:36555310-36932613	1.37	50.55	69.47	0.0000	0.0000
ENSG00000251587	LDHAP1	chr4:4895908-4896900	1.37	25.34	34.76	0.0000	0.0006
ENSG00000145088	EAF2	chr3:121554029-121605373	1.37	34.00	46.63	0.0000	0.0000
ENSG00000172081	MOB3A	chr19:2071036-2096269	1.37	52.90	72.55	0.0000	0.0000
ENSG00000197324	LRP10	chr14:23340821-23350789	1.37	34.45	47.24	0.0001	0.0048
ENSG00000228080	HLA-DRB1	chr6_ssto_hap7:3850430-4111880	1.37	103.26	141.28	0.0000	0.0000
ENSG00000128040	SPINK2	chr4:57676025-57687908	1.36	19.08	25.94	0.0004	0.0209
ENSG00000125772	GPCPD1	chr20:5525084-5591672	1.35	39.26	53.18	0.0001	0.0056
ENSG00000081189	MEF2C	chr5:87803362-88762215	1.35	52.98	71.43	0.0000	0.0000
ENSG00000112972	HMGCS1	chr5:43287702-43313614	1.35	167.15	225.30	0.0000	0.0000
ENSG00000196923	PDLIM7	chr5:176910394-176938275	1.35	35.66	48.06	0.0000	0.0013
ENSG00000001630	CYP51A1	chr7:91741464-91810039	1.35	32.91	44.29	0.0000	0.0020
ENSG00000159840	ZYX	chr7:143078172-143220542	1.34	37.08	49.76	0.0001	0.0048
ENSG00000188765	TMSB4XP2	chr2:3642425-3692048	1.34	1022.50	1369.26	0.0009	0.0388
ENSG00000226417	CLIC1	chr6_mcf_hap5:3008685-3199991	1.34	27.76	37.16	0.0000	0.0000
ENSG00000226248	CLIC1	chr6_dbb_hap3:2980383-2993114	1.34	27.67	36.99	0.0000	0.0000
ENSG00000230685	CLIC1	chr6_cox_hap2:3204431-3217149	1.34	27.69	36.99	0.0000	0.0000
ENSG00000223639	CLIC1	chr6_ssto_hap7:3025631-3038358	1.34	27.69	36.99	0.0000	0.0000
ENSG00000206394	CLIC1	chr6_qbl_hap6:2988444-3001178	1.34	27.68	36.98	0.0000	0.0000
ENSG00000027697	IFNGR1	chr6:137518620-137540586	1.34	27.61	36.88	0.0000	0.0004
ENSG00000226651	CLIC1	chr6_mann_hap4:2971895-3163173	1.34	27.81	37.13	0.0000	0.0000
ENSG00000213719	CLIC1	chr6:31694814-31707540	1.33	27.72	36.98	0.0000	0.0000

ENSG00000236090	LDHAP3	chr2:42046886-42047894	1.33	25.97	34.64	0.0000	0.0027
ENSG00000131196	NFATC1	chr18:77155771-77289325	1.33	31.76	42.30	0.0000	0.0000
ENSG00000225855	RUSC1-AS1	chr1:155278538-155300905	1.33	12.88	17.15	0.0009	0.0377
ENSG00000185607	ACTBP7	chr15:44162961-44487450	1.33	11.08	14.72	0.0011	0.0459
ENSG00000172175	MALT1	chr18:56338617-56421130	1.32	17.57	23.28	0.0000	0.0000
ENSG00000206240	HLA-DRB1	chr6_cox_hap2:3998150-4028758	1.32	214.60	284.18	0.0000	0.0000
ENSG00000206306	HLA-DRB1	chr6_qbl_hap6:3784599-3815217	1.32	214.60	284.18	0.0000	0.0000
ENSG00000163219	ARHGAP25	chr2:68906732-69053965	1.32	33.68	44.49	0.0000	0.0012
ENSG00000107140	TESK1	chr9:35605366-35647096	1.32	50.48	66.47	0.0000	0.0000
ENSG00000235674	LDHAP2	chr1:235824340-236046940	1.32	50.00	65.75	0.0000	0.0005
ENSG00000214110	LDHAP4	chr9:14921334-14922332	1.31	210.58	276.09	0.0000	0.0000
ENSG00000067064	IDI1	chr10:1034337-1095110	1.31	100.10	130.86	0.0000	0.0000
ENSG00000138756	BMP2K	chr4:79697495-79860592	1.31	40.34	52.71	0.0000	0.0001
ENSG00000227671	MIR3916	chr1:247353152-247372795	1.31	25.01	32.66	0.0000	0.0000
ENSG00000152256	PDK1	chr2:173292081-173489823	1.30	36.41	47.51	0.0004	0.0221
ENSG00000235847	LDHAP7	chr2:84743578-85046713	1.30	48.15	62.76	0.0000	0.0012
ENSG00000007944	MYLIP	chr6:16129355-16148479	1.30	12.88	16.72	0.0000	0.0005
ENSG00000112343	TRIM38	chr6:25963029-25985348	1.30	8.83	11.45	0.0000	0.0029
ENSG00000175105	ZNF654	chr3:88101093-88217879	1.30	3.00	3.90	0.0008	0.0373
ENSG00000102144	PGK1	chrX:77320684-77384793	1.30	659.51	854.94	0.0000	0.0000
ENSG00000186480	INSIG1	chr7:155089485-155101945	1.30	278.05	360.10	0.0000	0.0000
ENSG00000213574	LDHAP5	chr10:120692185-120692807	1.29	100.13	129.62	0.0000	0.0012
ENSG00000105287	PRKD2	chr19:47150868-47220384	1.29	19.29	24.96	0.0000	0.0000
ENSG00000162927	PUS10	chr2:61169103-61276394	1.29	9.97	12.88	0.0000	0.0026
ENSG00000257473	HLA-DQA2	chr6_cox_hap2:4055570-4061793	1.29	94.49	121.63	0.0000	0.0000
ENSG00000206305	HLA-DQA1	chr6_qbl_hap6:3841980-3848260	1.29	98.01	126.08	0.0000	0.0000
ENSG00000104765	BNIP3L	chr8:26236774-26371608	1.28	33.08	42.33	0.0007	0.0321
ENSG00000101608	MYL12A	chr18:3247478-3261848	1.28	149.26	190.74	0.0000	0.0000
ENSG00000223551	TMSB4XP4	chr9:131102924-131123502	1.28	58.80	75.11	0.0003	0.0152
ENSG00000187653	TMSB4XP8	chr4:91048685-92523064	1.28	4409.61	5630.75	0.0002	0.0110
ENSG00000213290	PGK1P2	chr19:12670384-12671919	1.28	46.19	58.97	0.0000	0.0021
ENSG00000099840	IZUMO4	chr19:2096379-2099592	1.28	29.86	38.08	0.0007	0.0302
ENSG00000179335	CLK3	chr15:74890840-74988633	1.28	110.22	140.54	0.0000	0.0004
ENSG00000162511	LAPTM5	chr1:31205315-31230667	1.27	172.57	219.90	0.0000	0.0000
ENSG00000109046	WSB1	chr17:25621101-25640657	1.27	64.39	81.97	0.0000	0.0023

ENSG00000170949	ZNF160	chr19:53569866-53606687	1.27	5.83	7.42	0.0001	0.0081
ENSG00000008282	SYPL1	chr7:105730948-105753022	1.27	87.36	111.13	0.0000	0.0000
ENSG00000137642	SORL1	chr11:121318039-121504387	1.27	30.67	38.99	0.0001	0.0087
ENSG00000133985	TTC9	chr14:71108503-71142077	1.27	15.52	19.70	0.0000	0.0007
ENSG00000147168	IL2RG	chrX:70327253-70331958	1.27	206.38	261.83	0.0001	0.0036
ENSG00000119403	PHF19	chr9:123617976-123639606	1.27	103.89	131.76	0.0000	0.0000
ENSG00000228612	HK2P1	chrX:79827369-79830106	1.27	7.99	10.12	0.0008	0.0364
ENSG00000205542	TMSB4X	chrX:12993226-12995346	1.26	1091.60	1380.31	0.0000	0.0000
ENSG00000184009	ACTG1	chr17:79476996-79494802	1.26	1584.63	2001.96	0.0000	0.0000
ENSG00000149781	FERMT3	chr11:63974149-64001824	1.26	279.36	352.84	0.0000	0.0000
ENSG00000156675	RAB11FIP1	chr8:37716135-37756985	1.26	10.06	12.69	0.0000	0.0022
ENSG00000214297	ALDOAP2	chr10:127262939-127371713	1.26	127.14	160.32	0.0000	0.0005
ENSG00000196352	CD55	chr1:207494852-207534311	1.26	25.22	31.79	0.0000	0.0015
ENSG00000081320	STK17B	chr2:196998289-197041227	1.26	67.00	84.31	0.0000	0.0016
ENSG00000236876	TMSB4XP1	chr1:42895999-43120335	1.26	4349.16	5468.48	0.0001	0.0070
ENSG00000196604	POTEF	chr2:130831107-130886795	1.26	6.91	8.68	0.0003	0.0161
ENSG00000167460	TPM4	chr19:16178316-16213813	1.25	74.12	92.96	0.0000	0.0003
ENSG00000230043	TMSB4XP6	chr20:49411430-49493714	1.25	10568.20	13242.60	0.0000	0.0031
ENSG00000121064	SCPEP1	chr17:55055465-55084129	1.25	61.98	77.66	0.0000	0.0020
ENSG00000149925	ALDOA	chr16:30064410-30081778	1.25	2056.86	2576.58	0.0000	0.0000
ENSG00000114023	FAM162A	chr3:122103022-122134882	1.25	90.07	112.70	0.0000	0.0001
ENSG00000134046	MBD2	chr18:51679078-51751158	1.25	340.32	425.66	0.0006	0.0282
ENSG00000228253	MT-ATP8	chrM:8365-9990	1.25	20644.20	25740.60	0.0000	0.0005
ENSG00000102393	GLA	chrX:100645811-100669121	1.25	33.32	41.52	0.0008	0.0373
ENSG00000181577	C6orf223	chr6:43963459-44045689	1.25	26.19	32.62	0.0001	0.0040

Table 3.3 Genes downregulated greater than 25% after treatment with polyamide **1** for 24 hours compared to non-treatment.

Ensembl Gene	Gene	Locus	Ratio	NT fpkm	GGGW fpkm	p_val	q_val
ENSG00000258486	RN7SL1	chr14:50043389-50081390	0.00	19.56	0.00	0.0001	0.0070
ENSG00000214189	ZNF788	chr19:12203077-12225499	0.08	0.86	0.07	0.0000	0.0020
ENSG00000176020	AMIGO3	chr3:49711434-49761384	0.27	1.64	0.44	0.0004	0.0204
ENSG00000165029	ABCA1	chr9:107543282-107691173	0.51	1.82	0.92	0.0000	0.0023
ENSG00000134250	NOTCH2	chr1:120454175-120612240	0.58	18.54	10.84	0.0012	0.0500
ENSG00000117016	RIMS3	chr1:41086350-41131329	0.60	17.81	10.61	0.0000	0.0000
ENSG00000155792	DEPTOR	chr8:120879658-121063152	0.60	10.15	6.08	0.0011	0.0469
ENSG00000073282	TP63	chr3:189349204-189615068	0.61	18.37	11.13	0.0000	0.0000
ENSG00000239899	RN7SL674P	chr2:11674241-11782914	0.62	201.82	124.57	0.0000	0.0000
ENSG00000137393	RNF144B	chr6:18366966-18469105	0.62	84.26	52.24	0.0000	0.0000
ENSG00000130775	THEMIS2	chr1:28199054-28213196	0.62	49.43	30.77	0.0000	0.0000
ENSG00000167483	FAM129C	chr19:17634109-17664647	0.63	3.34	2.09	0.0002	0.0094
ENSG00000244642	RN7SL396P	chr8:120874901-120875181	0.64	238.82	153.89	0.0000	0.0000
ENSG00000211640	IGLV6-57	chr22:22550112-22550686	0.65	44.34	28.60	0.0000	0.0006
ENSG00000230006	ANKRD36BP2	chr2:89065323-89106126	0.65	38.78	25.07	0.0001	0.0075
ENSG00000239437	RN7SL752P	chr3:129274017-129325661	0.65	135.52	87.77	0.0000	0.0002
ENSG00000125089	SH3TC1	chr4:8183798-8243530	0.65	79.36	51.46	0.0000	0.0000
ENSG00000265735	RN7SL5P	chr9:8314245-10612723	0.65	1756.91	1144.65	0.0000	0.0000
ENSG00000101144	BMP7	chr20:55743803-55841685	0.66	110.79	72.68	0.0002	0.0118
ENSG00000240869	RN7SL128P	chr6:20402397-20493941	0.66	260.67	172.73	0.0000	0.0000
ENSG00000082438	COBLL1	chr2:165510133-165705844	0.66	30.06	19.98	0.0002	0.0111
ENSG00000263740	RN7SL4P	chr3:15708742-15901278	0.67	1621.44	1088.28	0.0000	0.0000
ENSG00000211895	IGHA1	chr14:106173456-106175002	0.67	15.32	10.29	0.0000	0.0006
ENSG00000101846	STS	chrX:7137496-7272851	0.67	5.14	3.47	0.0000	0.0000
ENSG00000163884	KLF15	chr3:126061477-126076285	0.68	9.27	6.26	0.0012	0.0482
ENSG00000264462	MIR3648-1	chr21:9825831-9826011	0.68	1496.82	1011.79	0.0000	0.0000
ENSG00000211897	IGHG3	chr14:106235438-106237742	0.68	13.25	8.98	0.0000	0.0009
ENSG00000160856	FCRL3	chr1:157644110-157670775	0.68	32.28	21.96	0.0003	0.0176
ENSG00000176533	GNG7	chr19:2511217-2702746	0.68	24.17	16.52	0.0000	0.0000
ENSG00000132970	WASF3	chr13:27131839-27263085	0.69	6.00	4.13	0.0000	0.0000
ENSG00000179873	NLRP11	chr19:56296769-56393218	0.70	4.17	2.90	0.0000	0.0002

ENSG00000145990	GFOD1	chr6:13358061-13487787	0.70	11.10	7.73	0.0000	0.0000
ENSG00000226958	RNA28S5	chrX:108297360-108297792	0.70	2581.19	1802.17	0.0000	0.0000
ENSG00000112182	BACH2	chr6:90636247-91006627	0.70	92.93	64.95	0.0000	0.0001
ENSG00000221963	APOL6	chr22:36044441-36057404	0.70	5.52	3.87	0.0000	0.0018
ENSG00000197256	KANK2	chr19:11274943-11308243	0.70	28.80	20.24	0.0000	0.0000
ENSG00000211896	IGHG1	chr14:106202679-106209408	0.70	120.97	85.27	0.0000	0.0000
ENSG00000116717	GADD45A	chr1:68150743-68154021	0.71	58.38	41.66	0.0000	0.0000
ENSG00000166428	PLD4	chr14:105391152-105399574	0.72	27.51	19.76	0.0002	0.0119
ENSG00000159842	ABR	chr17:906757-1132315	0.72	234.84	168.72	0.0000	0.0000
ENSG00000211893	IGHG2	chr14:106109388-106115394	0.72	12.84	9.25	0.0010	0.0416
ENSG00000160505	NLRP4	chr19:56296769-56393218	0.72	6.00	4.33	0.0000	0.0003
ENSG00000175040	CHST2	chr3:142838172-142841800	0.72	10.68	7.71	0.0000	0.0001
ENSG00000155966	AFF2	chrX:147582138-148082193	0.72	9.50	6.88	0.0000	0.0005
ENSG00000221930	FAM45B	chrX:129611042-129658231	0.73	12.32	8.93	0.0009	0.0389
ENSG00000054654	SYNE2	chr14:64319682-64805317	0.73	183.41	133.35	0.0000	0.0000
ENSG00000168016	TRANK1	chr3:36868310-36986548	0.73	62.79	45.67	0.0000	0.0017
ENSG00000169750	RAC3	chr17:79989499-79992080	0.73	26.90	19.64	0.0000	0.0022
ENSG00000211892	IGHG4	chr14:106090686-106092403	0.73	18.42	13.53	0.0002	0.0097
ENSG00000164691	TAGAP	chr6:159455499-159466184	0.73	14.62	10.74	0.0000	0.0001
ENSG00000105327	BBC3	chr19:47724078-47736023	0.74	9.86	7.26	0.0001	0.0084
ENSG00000184384	MAML2	chr11:95709761-96076382	0.74	1.99	1.47	0.0008	0.0346
ENSG00000149639	SOGA1	chr20:35405844-35492089	0.74	12.62	9.33	0.0000	0.0000
ENSG00000149418	ST14	chr11:130029456-130080356	0.74	60.33	44.74	0.0000	0.0000
ENSG00000254709	IGLL5	chr22:23229959-23238014	0.74	354.62	263.92	0.0000	0.0000
ENSG00000117148	ACTL8	chr1:18081807-18153558	0.75	19.18	14.29	0.0000	0.0013
ENSG00000185838	GNB1L	chr22:19744225-19842462	0.75	24.82	18.51	0.0005	0.0237
ENSG00000211978	IGHV5-78	chr14:107259337-107259632	0.75	237.09	177.14	0.0001	0.0059
ENSG00000065057	NTHL1	chr16:2089815-2185899	0.75	98.92	73.91	0.0000	0.0000
ENSG00000135144	DTX1	chr12:113494513-113535833	0.75	413.55	309.92	0.0000	0.0000
ENSG00000088305	DNMT3B	chr20:31350190-31397162	0.75	7.95	5.97	0.0001	0.0047
ENSG00000128965	CHAC1	chr15:41245159-41248710	0.75	18.76	14.09	0.0005	0.0250
ENSG00000119139	TJP2	chr9:71736208-71870124	0.75	25.64	19.26	0.0006	0.0266
ENSG00000184524	CEND1	chr11:787103-790123	0.75	51.17	38.56	0.0004	0.0221

Table 3.4 Genes upregulated greater than 25% after treatment with polyamide **2** for 24 hours compared to non-treatment.

Ensembl Gene	Gene	Locus	Ratio	NT fpkm	GWWC fpkm	p_val	q_val
ENSG00000125675	GRIA3	chrX:122318005-122624766	N/A	0.00	1.30	0.0000	0.0025
ENSG00000164076	CAMKV	chr3:49895420-49907655	N/A	0.00	2.94	0.0000	0.0000
ENSG00000070808	CAMK2A	chr5:149569519-149669854	N/A	0.00	0.61	0.0000	0.0006
ENSG00000154188	ANGPT1	chr8:108261720-108510283	N/A	0.00	0.50	0.0000	0.0024
ENSG00000127152	BCL11B	chr14:99635623-99737861	16.50	0.07	1.14	0.0000	0.0000
ENSG00000239527	RPS23P7	chr17:60447578-60493837	10.63	0.54	5.69	0.0001	0.0050
ENSG00000253556	MTCO1P4	chr8:104101023-104102899	9.79	0.10	1.00	0.0003	0.0148
ENSG00000214204	HNRNPA1P43	chr1:116399481-116400440	5.03	0.30	1.50	0.0006	0.0293
ENSG00000101335	MYL9	chr20:34894257-35274619	3.91	0.33	1.30	0.0005	0.0260
ENSG00000213704	EEF1A1P15	chrX:97644507-97645918	3.78	0.79	2.98	0.0000	0.0000
ENSG00000188042	ARL4C	chr2:235401684-235405697	3.32	0.15	0.48	0.0002	0.0094
ENSG00000081059	TCF7	chr5:133450401-133487556	3.22	2.74	8.83	0.0000	0.0002
ENSG00000213128	RPL32P31	chr17:78516002-78516405	3.19	2.12	6.76	0.0010	0.0421
ENSG00000197956	S100A6	chr1:153506078-153508720	3.10	5.91	18.33	0.0000	0.0000
ENSG00000237882	PPIAP13	chr10:76849005-76849483	2.83	2.56	7.24	0.0002	0.0110
ENSG00000200312	RN7SKP255	chr14:89591214-90421121	2.16	18.53	40.03	0.0000	0.0005
ENSG00000200488	RN7SKP203	chr2:76672204-76672536	2.07	20.64	42.74	0.0000	0.0001
ENSG00000202198	RN7SK	chr6:52860417-52860748	1.90	83.52	158.42	0.0000	0.0000
ENSG00000201428	RN7SKP71	chr12:112597991-112819896	1.76	31.94	56.11	0.0000	0.0015
ENSG00000186834	HEXIM1	chr17:43224683-43236822	1.40	5.98	8.35	0.0000	0.0000
ENSG00000176393	RNPEP	chr1:201951499-201986316	1.26	88.42	111.35	0.0000	0.0005

Table 3.5 Genes downregulated greater than 25% after treatment with polyamide **2** for 24 hours compared to non-treatment.

Ensembl Gene ID	Gene	Locus	Ratio	NT fpkm	GWWC fpkm	p_val	q_val
ENSG00000260280	SLX1B-SULT1A4	chr16:29262828-29606395	0.00	1.58	0.00	0.0000	0.0001
ENSG00000134532	SOX5	chr12:23682439-24103966	0.44	17.01	7.56	0.0000	0.0013
ENSG00000131374	TBC1D5	chr3:17199898-18568819	0.45	18.98	8.54	0.0000	0.0000
ENSG00000184903	IMMP2L	chr7:110303109-111202573	0.49	15.84	7.81	0.0002	0.0121
ENSG00000131558	EXOC4	chr7:132937828-133751342	0.51	99.41	50.51	0.0000	0.0000
ENSG00000145996	CDKAL1	chr6:20534687-21232635	0.57	7.13	4.04	0.0000	0.0011
ENSG00000139734	DIAPH3	chr13:60239716-60738119	0.61	7.93	4.83	0.0000	0.0000
ENSG00000119522	DENND1A	chr9:126118448-126692431	0.62	45.22	27.97	0.0000	0.0003
ENSG00000073282	TP63	chr3:189349204-189615068	0.64	18.37	11.68	0.0000	0.0000
ENSG00000164808	SPIDR	chr8:48173166-48648868	0.64	128.25	82.62	0.0000	0.0000
ENSG00000155966	AFF2	chrX:147582138-148082193	0.65	9.50	6.16	0.0000	0.0000
ENSG00000112699	GMDS	chr6:1624040-2245926	0.65	33.89	22.14	0.0001	0.0037
ENSG00000141627	DYM	chr18:46550072-46987717	0.66	58.64	38.58	0.0000	0.0001
ENSG00000111880	RNGTT	chr6:89319984-89673348	0.67	12.09	8.10	0.0000	0.0000
ENSG00000133195	SLC39A11	chr17:70642087-71088851	0.67	42.03	28.21	0.0000	0.0007
ENSG00000049323	LTBP1	chr2:33172038-33624576	0.67	23.00	15.48	0.0003	0.0138
ENSG00000198846	TOX	chr8:59717976-60033905	0.68	4.89	3.31	0.0000	0.0001
ENSG00000170396	ZNF804A	chr2:185463092-185804219	0.68	4.11	2.80	0.0000	0.0002
ENSG00000144535	DIS3L2	chr2:232825954-233209060	0.68	21.08	14.37	0.0004	0.0190
ENSG00000156110	ADK	chr10:75910959-76469061	0.68	38.74	26.51	0.0000	0.0000
ENSG00000167216	KATNAL2	chr18:44526786-44628613	0.69	3.13	2.16	0.0009	0.0397
ENSG00000184384	MAML2	chr11:95709761-96076382	0.69	1.99	1.38	0.0001	0.0069
ENSG00000184220	CMSS1	chr3:99536677-99897447	0.69	88.52	61.50	0.0000	0.0000
ENSG00000091157	WDR7	chr18:54318615-54698828	0.70	3.61	2.51	0.0000	0.0000
ENSG00000174891	RSRC1	chr3:157813742-158288855	0.70	23.63	16.44	0.0000	0.0017
ENSG00000259660	DNM1P47	chr15:102291234-102334505	0.70	0.60	0.42	0.0009	0.0391
ENSG00000137393	RNF144B	chr6:18366966-18469105	0.70	84.26	58.92	0.0000	0.0000
ENSG00000152061	RABGAP1L	chr1:174084437-174964445	0.70	93.94	65.86	0.0000	0.0000
ENSG00000185104	FAF1	chr1:50905149-51425935	0.70	65.35	45.88	0.0000	0.0000
ENSG00000153317	ASAP1	chr8:131064352-131455906	0.71	29.49	20.80	0.0007	0.0306
ENSG00000049618	ARID1B	chr6:157099062-157530401	0.71	24.14	17.20	0.0000	0.0000

ENSG00000182247	UBE2E2	chr3:23244510-23633284	0.71	29.49	21.03	0.0000	0.0004
ENSG00000117090	SLAMF1	chr1:160577889-160617085	0.71	27.01	19.30	0.0000	0.0003
ENSG00000138623	SEMA7A	chr15:74701629-74726808	0.72	22.73	16.31	0.0010	0.0431
ENSG00000054654	SYNE2	chr14:64319682-64805317	0.72	183.41	131.71	0.0000	0.0000
ENSG00000153015	CWC27	chr5:64064756-64314418	0.72	24.69	17.79	0.0000	0.0027
ENSG00000197157	SND1	chr7:127292233-127732661	0.73	610.24	446.33	0.0000	0.0000
ENSG00000155849	ELMO1	chr7:36893960-37488852	0.73	86.24	63.11	0.0000	0.0000
ENSG00000005810	MYCBP2	chr13:77618791-77901185	0.73	82.32	60.25	0.0000	0.0005
ENSG00000176463	SLCO3A1	chr15:92396924-92874267	0.73	41.59	30.47	0.0010	0.0411
ENSG00000156639	ZFAND3	chr6:37787274-38122400	0.73	32.89	24.13	0.0007	0.0309
ENSG00000038382	TRIO	chr5:14143810-14532235	0.74	103.50	76.21	0.0003	0.0138
ENSG00000010803	SCMH1	chr1:41492871-41707826	0.74	57.57	42.68	0.0010	0.0416
ENSG00000235823	LINC00263	chr10:102133371-102143125	0.74	5.92	4.41	0.0008	0.0338
ENSG00000075151	EIF4G3	chr1:21132971-21503377	0.74	111.99	83.41	0.0000	0.0000
ENSG00000144645	OSBPL10	chr3:31699381-32119072	0.75	112.81	84.50	0.0000	0.0001
ENSG00000198648	STK39	chr2:168810529-169104651	0.75	21.20	15.90	0.0003	0.0170
ENSG00000145349	CAMK2D	chr4:114372187-114683083	0.75	39.19	29.50	0.0001	0.0079

3.6 References

(1) Dunn, G. P.; Old, L. J.; Schreiber, R. D. *Annu. Rev. Immunol.* **2004**, *22*, 329-360.

(2) Hanahan, D.; Weinberg, R. A. *Cell.* **2011**, *144*, 646-674.

(3) Dunn, G. P.; Old, L. J.; Schreiber, R. D. *Immunity.* **2004**, *21*, 137-148.

(4) Koebel, C. M.; Vermi, W.; Swann, J. B.; Zerafa, N.; Rodig, S. J.; Old, L. J.; Smyth, M. J.; Schreiber, R. D. *Nature.* **2007**, *450*, 903-907.

(5) Schreiber, R. D.; Old, L. J.; Smyth, M. J. *Science Signalling.* **2011**, *331*, 1565.

(6) O'Sullivan, T.; Saddawi-Konefka, R.; Vermi, W.; Koebel, C. M.; Arthur, C.; White, J. M.; Uppaluri, R.; Andrews, D. M.; Ngiow, S. F.; Teng, M. W.; Smyth, M. J.; Schreiber, R. D.; Bui, J. D. *J. Exp. Med.* **2012**, *209*, 1869-1882.

(7) Eggermont, A.; Robert, C.; Soria, J. C.; Zitvogel, L. *Oncoimmunology.* **2014**, *3*, e27560.

(8) Matzinger, P. *Science.* **2002**, *296*, 301-305.

(9) Obeid, M.; Tesniere, A.; Ghiringhelli, F.; Fimia, G. M.; Apetoh, L.; Perfettini, J. L.; Castedo, M.; Mignot, G.; Panaretakis, T.; Casares, N.; Métivier, D.; Larochette, N.; van Endert, P.; Ciccosanti, F.; Piacentini, M.; Zitvogel, L.; Kroemer, G. *Nat. Med.* **2007**, *13*, 54-61.

(10) Jaiswal, S.; Chao, M. P.; Majeti, R.; Weissman, I. L. *Trends. Immunol.* **2010**, *31*, 212-219.

(11) Tseng, D.; Volkmer, J. P.; Willingham, S. B.; Contreras-Trujillo, H.; Fathman, J. W.; Fernhoff, N. B.; Seita, J.; Inlay, M. A.; Weiskopf, K.; Miyanishi, M.; Weissman, I. L. *Proc. Natl. Acad. Sci. U. S. A.* **2013**, *110*, 11103-11108.

(12) Zitvogel, L.; Apetoh, L.; Ghiringhelli, F.; Kroemer, G. *Nat. Rev. Immunol.* **2008**, *8*, 59-73.

(13) Zitvogel, L.; Kepp, O.; Kroemer, G. *Cell.* **2010**, *140*, 798-804.

(14) Kepp, O.; Galluzzi, L.; Martins, I.; Schlemmer, F.; Adjemian, S.; Michaud, M.; Sukkurwala, A. Q.; Menger, L.; Zitvogel, L.; Kroemer, G. *Cancer Metastasis Rev.* **2011**, *30*, 61-69.

(15) Chao, M. P.; Jaiswal, S.; Weissman-Tsukamoto, R.; Alizadeh, A. A.; Gentles, A. J.; Volkmer, J.; Weiskopf, K.; Willingham, S. B.; Raveh, T.; Park, C. Y.; Majeti, R.; Weissman, I. L. *Sci. Transl. Med.* **2010**, *2*, 63ra94.

(16) Idzko, M.; Dichmann, S.; Ferrari, D.; Di Virgilio, F.; la Sala, A.; Giampiero, G.; Panther, E.; Norgauer, J. *Blood.* **2002**, *100*, 925-932.

(17) Aymeric, L.; Apetoh, L.; Ghiringhelli, F.; Tesniere, A.; Martins, I.; Kroemer, G.; Smyth, M. J.; Zitvogel, L. *Cancer Res.* **2010**, *70*, 855-858.

(18) Rovere-Querini, P.; Capobianco, A.; Scaffidi, P.; Valentinis, B.; Catalanotti, F.; Giazzon, M.; Dumitriu, I. E.; Müller, S.; Iannacone, M.; Traversari, C.; Bianchi, M. E.; Manfredi, A. A. *EMBO reports.* **2004**, *5*, 825-830.

(19) Guerriero, . L.; Ditsworth, D.; Catanzaro, . M.; Sabino, G.; Furie, . B.; Kew, . R.; Crawford, . C.; Zong, -X. *J. Immunol.* **2011**, *186*, 3517-3526.

(20) Gasser, S.; Orsulic, S.; Brown, E. J.; Raulet, D. H. *Nature.* **2005**, *436*, 1186-1190.

(21) Wade, W. S.; Mrksich, M.; Dervan, P. B. *J. Am. Chem. Soc.* **1992**, *114*, 8783-8794.

(22) Trauger, J. W.; Baird, E. E.; Dervan, P. B. *Nature.* **1996**, *382*, 559-561.

(23) White, S.; Baird, E. E.; Dervan, P. B. *Chem. Biol.* **1997**, *4*, 569-578.

(24) White, S.; Szewczyk, J. W.; Turner, J. M.; Baird, E. E.; Dervan, P. B. *Nature.* **1998**, *391*, 468-471.

(25) Kielkopf, C. L.; Baird, E. E.; Dervan, P. B.; Rees, D. C. *Nat. Struct. Biol.* **1998**, *5*, 104-109.

(26) Kielkopf, C. L.; White, S.; Szewczyk, J. W.; Turner, J. M.; Baird, E. E.; Dervan, P. B.; Rees, D. C. *Science.* **1998**, *282*, 111-115.

(27) Dervan, P. B.; Edelson, B. S. *Curr. Opin. Struct. Biol.* **2003**, *13*, 284-299.

(28) Mrksich, M.; Parks, M. E.; Dervan, P. B. *J. Am. Chem. Soc.* **1994**, *116*, 7983-7988.

(29) Hsu, C. F.; Phillips, J. W.; Trauger, J. W.; Farkas, M. E.; Belitsky, J. M.; Heckel, A.; Olenyuk, B. Z.; Puckett, J. W.; Wang, C. C.; Dervan, P. B. *Tetrahedron.* **2007**, *63*, 6146-6151.

(30) Nickols, N. G.; Jacobs, C. S.; Farkas, M. E.; Dervan, P. B. *ACS Chem. Biol.* **2007**, *2*, 561-571.

(31) Nickols, N. G.; Dervan, P. B. *Proc. Natl. Acad. Sci. U. S. A.* **2007**, *104*, 10418-10423.

(32) Raskatov, J. A.; Meier, J. L.; Puckett, J. W.; Yang, F.; Ramakrishnan, P.; Dervan, P. B. *Proc. Natl. Acad. Sci. U. S. A.* **2012**, *109*, 1023-1028.

(33) Yang, F.; Nickols, N. G.; Li, B. C.; Marinov, G. K.; Said, J. W.; Dervan, P. B. *Proc. Natl. Acad. Sci. U. S. A.* **2013**, *110*, 1863-1868.

(34) Swalley, S. E.; Baird, E. E.; Dervan, P. B. *J. Am. Chem. Soc.* **1996**, *118*, 8198-8206.

(35) Nickols, N. G.; Szablowski, J. O.; Hargrove, A. E.; Li, B. C.; Raskatov, J. A.; Dervan, P. B. *Mol. Cancer Ther.* **2013**, *12*, 675-684.

(36) Kang, J. S.; Meier, J. L.; Dervan, P. B. *J. Am. Chem. Soc.* **2014**, *136*, 3687-3694.

(37) Martínez, T. F.; Phillips, J. W.; Karanja, K. K.; Polaczek, P.; Wang, C. -M.; Li, B. C.; Campbell, J. L.; Dervan, P. B. *Nucleic Acids Res.* **2015**, *42*, 11546-11559.

(38) Michalak, M.; Groenendyk, J.; Szabo, E.; Gold, L. I.; Opas, M. *Biochem. J.* **2009**, *417*, 651-666.

(39) Tufi, R.; Panaretakis, T.; Bianchi, K.; Criollo, A.; Fazi, B.; Di Sano, F.; Tesniere, A.; Kepp, O.; Paterlini-Brechot, P.; Zitvogel, L.; Piacentini, M.; Szabadkai, G.; Kroemer, G. *Cell Death Differ.* **2008**, *15*, 274-282.

(40) Peters, L. R.; Raghavan, M. *J. Immunol.* **2011**, *187*, 919-931.

(41) Maeshima, K.; Janssen, S.; Laemmli, U. K. *EMBO J.* **2001**, *20*, 3218-3228.

(42) Kawamoto, Y.; Bando, T.; Kamada, F.; Li, Y.; Hashiya, K.; Maeshima, K.; Sugiyama, H. *J. Am. Chem. Soc.* **2013**, *135*, 16468-16477.

(43) Meier, J. L.; Yu, A. S.; Korf, I.; Segal, D. J.; Dervan, P. B. *J. Am. Chem. Soc.* **2012**, *134*, 17814-17822.

(44) Pilch, D. S.; Poklar, N.; Gelfand, C. A.; Law, S. M.; Breslauer, K. J.; Baird, E. E.; Dervan, P. B. *Proc. Natl. Acad. Sci. U. S. A.* **1996**, *93*, 8306-8311.

(45) Panaretakis, T.; Kepp, O.; Brockmeier, U.; Tesniere, A.; Bjorklund, A. C.; Chapman, D. C.; Durchschlag, M.; Joza, N.; Pierron, G.; van Endert, P.; Yuan, J.; Zitvogel, L.; Madeo, F.; Williams, D. B.; Kroemer, G. *EMBO J.* **2009**, *28*, 578-590.

(46) Lippincott-Schwartz, J.; Yuan, L. C.; Bonifacino, J. S.; Klausner, R. D. *Cell.* **1989**, *56*, 801-813.

(47) Kaczmarek, A.; Vandenabeele, P.; Krysko, D. V. *Immunity.* **2013**, *38*, 209-223.

(48) Rubartelli, A.; Lotze, M. T. *Trends Immunol.* **2007**, *28*, 429-436.

(49) Mortazavi, A.; Williams, B. A.; McCue, K.; Schaeffer, L.; Wold, B. *Nat. Methods.* **2008**, *5*, 621-628.

(50) Langmead, B.; Trapnell, C.; Pop, M.; Salzberg, S. L. *Genome Biol.* **2009**, *10*, R25.

(51) Trapnell, C.; Pachter, L.; Salzberg, S. L. *Bioinformatics.* **2009**, *25*, 1105-1111.

(52) Trapnell, C.; Williams, B. A.; Pertea, G.; Mortazavi, A.; Kwan, G.; van Baren, M. J.; Salzberg, S. L.; Wold, B. J.; Pachter, L. *Nat. Biotechnol.* **2010**, *28*, 511-515.

(53) Balkwill, F. *Nat. Rev. Cancer.* **2009**, *9*, 361-371.

(54) Braud, V. M.; Allan, D. S.; O'Callaghan, C. A.; Söderström, K.; D'Andrea, A.; Ogg, G. S.; Lazetic, S.; Young, N. T.; Bell, J. I.; Phillips, J. H. *Nature.* **1998**, *391*, 795-799.

(55) Nuchtern, J. G.; Biddison, W. E.; Klausner, R. D. *Nature.* **1990**, *343*, 74-76.

(56) Neefjes, J.; Jongsma, M. L.; Paul, P.; Bakke, O. *Nat. Rev. Immunol.* **2011**, *11*, 823-836.

(57) Sukhatme, V. P.; Cao, X.; Chang, L. C.; Tsai-Morris, C. -H.; Stamenkovich, D.; Ferreira, P. C.; Cohen, D. R.; Edwards, S. A.; Shows, T. B.; Curran, T. *Cell.* **1988**, *53*, 37-43.

(58) McMahon, A. P.; Champion, J. E.; McMahon, J. A.; Sukhatme, V. P. *Development.* **1990**, *108*, 281-287.

(59) Seiler, M. P.; Mathew, R.; Liszewski, M. K.; Spooner, C. J.; Spooner, C.; Barr, K.; Meng, F.; Singh, H.; Bendelac, A. *Nat. Immunol.* **2012**, *13*, 264-271.

(60) Peck, D.; Crawford, E. D.; Ross, K. N.; Stegmaier, K.; Golub, T. R.; Lamb, J. *Genome Biol.* **2006**, *7*, R61.

(61) Kumar, S.; Boehm, J.; Lee, J. C. *Nat. Rev. Drug. Discov.* **2003**, *2*, 717-726.

(62) Liebermann, D. A.; Hoffman, B. *J. Mol. Signal.* **2008**, *3*, 15.

(63) Yamamoto, M.; Sato, S.; Hemmi, H.; Sanjo, H.; Uematsu, S.; Kaisho, T.; Hoshino, K.; Takeuchi, O.; Kobayashi, M.; Fujita, T.; Takeda, K.; Akira, S. *Nature.* **2002**, *420*, 324-329.

(64) Gough, D. J.; Messina, N. L.; Clarke, C. J.; Johnstone, R. W.; Levy, D. E. *Immunity.* **2012**, *36*, 166-174.

(65) Baird, E. E.; Dervan, P. B. *J. Am. Chem. Soc.* **1996**, *118*, 6141-6146.

(66) Puckett, J. W.; Green, J. T.; Dervan, P. B. *Org. Lett.* **2012**, *14*, 2774-2777.